Performance Evaluation of Carbon Dioxide Sequestration in Bubble Column Reactor using Fine/Micro Bubbles

By: Abas Siraj Hamda

A Thesis Submitted to

The Department of Chemical Engineering

School of Mechanical, Chemical and Materials Engineering

Presented in Partial Fulfillment of the Requirement for the Degree of Master's in Chemical Engineering (Specialization in Process Engineering)

Office of Graduate Studies

Adama Science and Technology University

Adama

March, 2021

Performance Evaluation of Carbon Dioxide Sequestration in Bubble Column Reactor using Fine/Micro Bubbles

By: Abas Siraj Hamda

Advisor: - Dr. Tatek Temesgen

Co-Advisor: - Dr. Mulugeta Yilma

A Thesis Submitted to

The Department of Chemical Engineering

School of Mechanical, Chemical and Materials Engineering

Presented in Partial Fulfillment of the Requirement for the Degree of Master's in Chemical Engineering (Specialization in Process Engineering)

Office of Graduate Studies

Adama Science and Technology University

Adama

March, 2021

Thesis approval sheet

We, the undersigned, members of the board of examiners of the final open defense by Abas Siraj Hamda have read and evaluated his thesis entitled "**Performance evaluation of carbon dioxide sequestration in bubble column reactor using fine/micro bubbles"** and examined the candidate. This is therefore, to certify that the thesis has been accepted in partial fulfillment of the requirement of the Degree of Master of Science in Chemical Engineering (Processing Engineering).

_____	_____	_____
Advisor	Signature	Date
_____	_____	_____
Co-Advisor	Signature	Date
_____	_____	_____
Chairperson	Signature	Date
_____	_____	_____
External Examiner	Signature	Date
_____	_____	_____
Internal Examiner	Signature	Date
_____	_____	_____
Head of Department	Signature	Date
_____	_____	_____
School Dead	Signature	Date
_____	_____	_____
Post Graduate Dead	Signature	Date

Declaration

I hereby declare that this MSc Thesis entitled "**Performance evaluation of carbon dioxide sequestration in bubble column reactor using fine/micro bubbles"** is my original work and has not been presented for a degree in any other university, and all sources of material used for this thesis have been duly acknowledged.

Name: Abas Siraj Hamda

Signature: _____

This MSc Thesis has been submitted for examination with my approval as thesis advisor.

Name: Dr. Tatek Temesgen

Signature: _____

Date of submission……

ACKNOWLEDGMENTS

First and foremost, ‘all praise is due to almighty God’ for his kindness and blessings, for his sailed me through the ups and downs, and ecstasies during this time. I express a deep sense of gratitude to my advisor Dr. Tatek Temesgen, for giving me the golden opportunity to work on this topic. I wish to thank him for his encouragement and support throughout my master thesis work which helped me overcome many obstacles. I feel very fortunate to have an opportunity to work under his advising. The load of enthusiasm and intensity he brings to the work is simply amazing. I would like to extend special thanks to my Co-Advisor Dr. Mulugeta Yilma for his valuable advice and comment on my work.

I wish to acknowledge the Mechanical Engineering workshop technicians Mr. Tajudin Ayub and Mr. Mokonen Girma for helping me with various technical issues and manufacturing of the equipment.

I take this opportunity to acknowledge and thank Adama Science and Technology University Chemical Engineering Department staffs, and laboratory technicians for their valuable assistance during laboratory work.

My thanks go to my employer, Haramaya University which grants me a tuition fee for my study program.

I express a deep sense of gratitude to my parents for their moral encouragement which put me on the right track to achieve the long way destiny.

Lastly, it is my heartfelt thanks go to my wife Soreti Abdela and my daughter Hikma Abas, for their understanding love, patience, and shouldering all the responsibilities. It is your greatest encouragement and sacrifices that brought this work to a successful end.

May Allah blessing all of you!

Abas Siraj Hamda

ASTU

March, 2021

TABLE OF CONTENTS

Contents Page

LIST OF TABLES

LIST OF FIGURES AND ILLUSTRATIONS

NOMENCLATURE

α	Specific interfacial area, m^2/m^3
A	Cross sectional area, m^2
C	Phase concentration, mole/L
D	Diameter of bubble column, m
D	Diameter of equivalent sphere, mm
d_{32}	Sauter mean diameter, mm
E	Enhancement factor
H	Height of bubble column, m
G	Acceleration gravity, m/s^2
K_g	Gas side mass transfer coefficient, kmol $m^{-2}s^{-1}kpa^{-1}$
K_l	Liquid side mass transfer coefficient, kmol $m^{-2}s^{-1}kpa^{-1}$
$K_l\alpha$	Overall Liquid side mass transfer coefficient, kmol $m^{-2}s^{-1}kpa^{-1}$
N_{CO2}	Mass transfer flux, Kmole m^{-2} s^{-1}
P	Total system pressure, kPa
Q	CO_2 flow rate, l min^{-1}
t	Time, sec
T	Temperature, ℃
W	Width of the column, m
U_g	Superficial gas velocity, cm/s
U_l	Superficial liquid velocity, cm/s
$Y_{CO2\ inlet}$	Mole fraction of inlet CO_2
$Y_{CO2\ out}$	Mole fraction of outlet CO_2
V	Velocity of venture, m^2

Z	Elevation, m

Greek Letters

ρ_l	Density of liquid, kg m^{-3}
ρ_g	Density of Gas, kg m^{-3}
α_{CO2}	CO_2 loading, mol /CO_2 mol solvent^{-1}
σ	Surface tension of liquid, N m−1
μ	Phase viscosity, kg m^{-1} s^{-1}
ε_g	Gas holdup
η_{CO2}	CO_2 Removal Efficiency

LIST OF ABBREVIATIONS

1-D	One Dimensional
2-D	Two Dimensional
3-D	Three Dimensional
ASTU	Adama science and Technology
BCR	Bubble Column Reactor
CCS	CO_2 Capture and Storage
DBS	Dual-Bubble-Size
DEA	Di-ethanolamine
EMMS	Energy-Minimization Multi-Scale
GHG	Green House Gases
MDEA	N-methyl Di-ethanolamine
MEA	Mono-ethanolamine
PDE	Partial Differential Equations
RTD	Residence Time Distributions
TEA	Tri-ethanolamine

ABSTRACT

Currently, carbon dioxide (CO_2) emissions are considered to be one of the major pollutants contributing to global greenhouse gas, causing the temperature of the atmosphere to rise and alter the radioactive balance of the earth. The main objective of this work is to evaluate performance of a lab scale mixed flow reactor and test the carbon dioxide absorption efficiency in the bubble column reactor using fine/microbubbles. In this work, the absorption of CO_2 using NH_3, NaOH and MEA solution were investigated experimentally in mixed flow bubble column reactor. The experiments were carried out at the solvents concentration range of 1 to 7% (v/v), and the CO_2 flow rate range of 1 to 2.5L/min. The performance of those solvents was compared in terms of the CO_2 removal efficiency. The experimental result showed that CO_2 removal efficiency of ammonia solution was maximum compared to all the three chemicals for both the conventional and microbubble support systems. Sodium hydroxide and Mono-ethanolamine solution take the next consecutive ranks respectively, under the operating condition of this work. The CO_2 removal efficiency of all the solvent increase with increasing the solvent concentration from 1 to 7% (V/V) and decrease with increasing the CO_2 flow rate from 1 to 2.5L/min. At the same time this works tried to investigate the effect of the bubble size on the CO_2 removal efficiency using micro-bubble assisted system and conventional bubble assisted system. It was found out that removal efficiency of all the solvents using micro-bubble assisted system was better than that of conventional bubble assisted system, because the smaller bubbles have a larger gas-liquid specific surface area.

Keywords: *Bubble column reactor; Splitter type micro-bubble generator; Carbon dioxide; Solvents; Removal Efficiency;* CO_2 *hold.*

CHAPTER ONE

INTRODUCTION

1.1. Background

Global warming caused by the increasing emission of greenhouse gases (GHG) is one of the most serious environmental issues all over the world [1,2]. Among the greenhouse gases, Carbon dioxide (CO_2) is regarded as one of the most important GHGs that have more contribution to global climate change, causing the temperature of the atmosphere to rise [1,2,3]. This anthropogenic CO_2 emission accounts for 80% of the total GHGs [1] and, it comes from fossil fuel utilization, especially from coal combustion.

Nowadays, the CO_2 concentration in the atmosphere has increased more than 39%, close to 400 ppm in May 2013. Which is significantly higher than the preindustrial level of about 280ppm to 300 ppm, with a corresponding increase in the global surface temperature of about 0.8℃ [4,5]. As estimated by [6], the global GHG emission in 2030 will increase by 25–90%, without climate change mitigation policies. Therefore, to mitigate the global GHG emission problem, the effort need to be focused on avoiding the production of carbon dioxide by reducing fossil fuel use [1] or removal of carbon dioxide from flue gases [2].

Various CO_2 capture methods have been intensively investigated for CO_2 capture from combustion flue gas, including chemical absorption methods, adsorption methods, cryogenic methods, separation using membranes and biological fixation, and the O_2/CO_2 combustion process [1, 5]. Among these technologies, the chemical absorption technology seems to be the most suitable technology to reduce CO_2 emission at the industrial application level due to its obvious advantages, e.g**.** high performance, high efficiency, and mature technology [2]. Chemical absorption methods for reducing CO_2 emission from fossil fuel that relies on the use of solvents. These absorbents are useful in removing CO_2 from several gas mixtures, among them natural gas, synthesis gas, and various refinery streams [7, 8]. Removal of CO_2 from gas streams by absorption processes widely uses aqueous solutions of alkanolamines, including Mono-ethanolamine (MEA) [9,10], di-ethanolamine (DEA) [11], tri-ethanolamine (TEA), and N-methyl di-ethanolamine (MDEA) [12], as the absorbents.

However, these solvents usually suffer the disadvantages of high energy requirement for regeneration, low absorption capacity limited at 0.4 kg of CO_2 per kg of absorbent, easy oxidization/degradation by SO_2 and O_2 in flue gas, and system corrosion [13], although they have better technical and economic feasibility than strong alkaline and their salt solutions (e.g., KOH, NaOH and Na_2CO_3) [2]. The choice of cost-effective and high-performance absorbent is still a very open and interesting question. Future research efforts should be directed toward developing better solvents for the removal of CO_2 with high CO_2 loading capacity and low regeneration energy [14].

Lately, aqueous solutions of NH_3 seem to be alternative solvents for removing CO_2 from flue gases [15]. Besides the general advantages such as high absorption efficiency [16], high absorption capacity [17], the low energy requirement for absorbent regeneration [1], and wide distribution of resources, aqueous ammonia could simultaneously remove SO_2, NO_x, and oxidized mercury [2,16]. Furthermore, the by-products, amine salts produced during the reaction of ammonia with CO_2, SO_2, and NO_x, can be used as fertilizer for soil improvement [2]. NaOH solution is also another alternative absorbent for CO_2 removal. Compared to the alkanolamines, the NaOH solution cannot be readily regenerated because $NaHCO_3$, the final product of CO_2 absorption to NaOH solution, is very soluble in an aqueous solution [18].

In addition to the solvent, it has been demonstrated that CO_2 capture performance was strongly affected by reaction conditions and reactor configurations. There are many contacting devices (reactor) that are used for CO_2 absorption such as packed column, bubble column, and spray column. Among these, the bubble column reactors (BCR) is one of the important compact multiphase reactors with high heat and mass transfer rates and low operation and maintenance costs, higher removal efficiency, and effective control of the liquid residence time that has been widely used in a variety of chemical and biochemical gas-liquid reaction systems [18,19,20].

The design of a bubble column reactor is based on the variation of parameters from an existing design with only minor redesign efforts involved for the improvement of an existing bubble column reactor [22]. More specifically, to design bubble column reactors, the following key factors such as gas hold-up, volumetric mass transfer coefficient, specific interfacial area, bubble size, and

kinetic rate constants, are fundamental for the proper design and the operational control of gas-liquid reactors [18,19].

In this study, the target is on the improvement of the removal efficiency of CO_2 by chemical absorption method using a solvent on fine/microbubbles based bubble column reactors, and examining the effects of operating parameters on CO_2 capture, and do comparison of different solvent performance in previous works.

1.2. Statement of the problems

Environmental protection is a critical issue worldwide, currently. In particular, CO_2 emissions are now considered to be one of the major pollutants contributing to global greenhouse gas, causing the temperature of the atmosphere to rise and alter the radioactive balance of the earth [3].

CO_2 is not toxic and one should not confuse it with highly toxic carbon monoxide. On the contrary, CO_2 increases plant growth as it provides, together with water, the basic materials needed for photosynthesis. The main problem of an increase in atmospheric CO_2-concentration is its shifting impact on the radiation balance of the atmosphere, the so-called "greenhouse" effect. This global warming effect has produced various weather anomalies such as powerful tropical storms, droughts, and floods with economic and health consequences. This causes dramatic global climatic and environmental changes.

The reduction of CO_2 concentration in the atmosphere is considered to be one of the most urgent requirements to reduce the global warming trend. Then for that reason, there is the need to develop and improve CO_2 sequestration technologies that are effective, stable, safe, and environmentally acceptable.

For the chemical absorption of CO_2 using chemical solvent the choice of cost-effective and high performance solvent is very open area, because of many solvents suffer several disadvantage such as low absorption capacity, high energy requirement and system corrosion. Based on these problems the effort should be focused on the developing of better solvents for CO_2 absorption with high absorption efficiency and low energy for regeneration.

1.3. Objectives

1.3.1. General objective

The main objective of this work is to evaluate performance of a lab scale mixed flow reactor and test the carbon dioxide absorption efficiency in the bubble column reactor using fine/microbubbles.

1.3.2. Specific objectives

The specific objectives are to: -

- ✓ Evaluate performance of mixed flow bubble column reactor for CO_2 absorption
- ✓ Test CO_2 capturing efficiency by using fine/microbubbles
- ✓ Examine the effects of operating parameters on CO_2 capture efficiency
- ✓ Compare capturing efficiency of the fine/microbubbles with the conventional bubbles

1.4. Significance of the study

The carbon dioxide emission at the global level can be have disastrous implications including global warming and see level rise. Researches such as this can play a very important role in mitigating these impact effectively and economically. As a result, some of the main beneficiaries of the outcome of this study are the Research community, Industries which has CO_2 emission, Environmental protection agencies and Adama science and technology university from the development of the gas-liquid reactor.

1.5. Scope of the study

To achieve the above-mentioned objective, the scope of this research is limited to designing, and manufacturing of a mixed flow bubble column reactor, and splitter type micro-bubble generator. After the reactor and the venture supported splitter type micro-bubble generator are manufactured and tested for the removal efficiency of carbon dioxide using fine/microbubbles. The effect of different parameters on the removal efficiency was conducted. Finally, the removal of carbon dioxide using fine/microbubble is compared to the conventional bubbles.

CHAPTER TWO

LITERATURE REVIEW

In this Chapter, literature review pertinent to this thesis is presented. It is divided into two part. In the first part, a brief review of the carbon dioxide properties, different approaches, and technologies of removing carbon dioxide emission, and chemical absorption mechanism are assessed. The second part reviews the designing of bubble column reactors, bubble properties and micro-bubble generation.

2.1. Carbon dioxide and its properties

Carbon dioxide is a trace gas. It is composed of one carbon atom covalently bonded to two oxygen atoms. Therefore, the geometry is linear. The carbon atom is at the center of the molecule. Thus, it is electrophilic [23]. Carbon dioxide which is deemed as acid gas forms an acidic solution (carbonic acid) when in contact with water.

However, it is less toxic and one should not confuse it with the highly toxic carbon monoxide. Besides that, CO_2 is also the primary GHG that is emitted as a result of human activities [23]. Due to certain human activities such as the combustion of fossil fuels, more CO_2 is being released uncontrollably into the atmosphere and thus resulting in global warming. On account of an increase in awareness regarding global warming, many technologies and researches are being done to reduce the amount of CO_2 that is being released into the environment.

2.2. Approaches to remove carbon dioxide emission into the atmosphere

There are different approaches to reduce CO_2 emissions into the atmosphere that are considered and adopted by various countries. These approaches include improve energy efficiency and promote energy conservation; increase usage of low carbon fuels, including natural gas, hydrogen, or nuclear power; deploy renewable energy, such as solar, wind, hydropower, and bioenergy; apply geoengineering approaches, e.g. afforestation and reforestation; and CO_2 capture and storage (CCS) [5, 23].

Amongst these different approaches to reducing CO_2 emissions, CCS can reduce CO_2 emissions (typically 85–90%) from large points of emission sources, such as power production utilities, and

energy-intensive emitters, e.g. cement kiln plants. In this approach, CO_2 is first captured from the flue/fuel gases, separated from the sorbent, transported, and then either stored permanently or reutilized industrially [5].

2.3. Carbon dioxide capture and sequestration technologies

CO_2 is formed during combustion and the type of combustion process directly affects the choice of an appropriate CO_2 removal process [5]. There are three main technologies to capturing the CO_2 generated from primary fossil fuel (coal, natural gas, or oil), biomass, or mixtures of these fuels depending on the processor power plant application in question [5, 24]. Namely post-combustion capture, pre-combustion capture, and oxy-fuel combustion capture. Within each capture process, several separation technologies can be employed as a standalone technology or coupled with other separation processes to capture CO_2 for sequestration.

2.3.1. Post-combustion Capture

In post-combustion CO_2 capturing technology, the CO_2 can be removed from the flue gas after combustion has taken place [5]. This technology is more appropriate for retrofitting existing power plants. Several methods exist for the post-combustion capture of CO_2 from flue gases [5, 25]. These include Absorptions, Adsorption, Membrane separation, Chemical looping combustion, and Cryogenic separation.

2.3.2. Pre-combustion capture

In pre-combustion CO_2 capturing technology, the fuels are first converted into a mixture of CO_2 and H_2 through a reforming (natural gas) or gasification (coal) process and the subsequent shift-reaction [5, 24]. CO_2 can be separated from the conversion product stream and H_2 can then be burned in a gas turbine or be used by the fuel cell. This technology is potentially less expensive than post-combustion capture [5, 25].

2.3.3. Oxy-fuel combustion

In oxy-fuel combustion CO_2 capturing technology, oxygen, instead of air, is used for combustion [25]. This can reduce the amount of nitrogen present in the exhaust gas that affects the subsequent separation process and the substantial reduction in thermal NOx is another advantage of this process [5].

Generally, the main Advantage and disadvantages of these three CO_2 capturing technology are summarized by [5] in the following table 2.1.

Table 2.1 Advantages and disadvantages of the three CO_2 capture technologies [5].

Capture process	**Application area**	**Advantages**	**Disadvantages**
Post-combustion	Coal-fired and gas-fired plants	Technology more mature than other alternatives; can easily retrofit into existing plants;	Low CO_2 concentration affects the capture efficiency
Pre-combustion	Coal-gasification plants	High CO_2 concentration enhance sorption efficiency; fully developed technology, commercially deployed at the required scale in some industrial sectors; opportunity for retrofit to existing plant;	Temperature associated heat transfer problem and efficiency decay issues associated with the use of hydrogen-rich gas turbine fuel; high parasitic power requirement for sorbent regeneration; inadequate experience due to few gasification plants currently operated in the market; high capital and operating costs for current sorption systems;
Oxy-fuel Combustion	Coal-fired and gas-fired plants	Very high CO_2 concentration that enhances absorption efficiency; mature air separation technologies available; the reduced volume of gas to be treated	High-efficiency drop and energy penalty; cryogenic O_2 production is costly; corrosion problem may arise;

2.4. Chemical absorption of carbon dioxide

Chemical absorption of CO_2 involves one or more reversible chemical reactions between CO_2 and another substance to produce a liquid or solid species that, upon heating, breaks down to liberate CO_2 and regenerate the material reacted with CO_2 [3]. Absorption is a transfer of a component in a gas phase into a liquid phase (solvent) where it is soluble in or it removes CO_2 from flue gas streams by contacting the flue gas with a solvent [27]. The interaction between the absorbed gas phases with the liquid phase where the gas dissolves is an important factor in the absorption process.

There are two types of absorption systems that are used to capture CO_2 based on the processes that are happening [11]. These are physical solvent-based absorption and chemical solvent-based absorption systems. Physical solvent-based absorption where the gas phase component is dissolved in the solvent and keeps its chemical integrity. The equilibrium concentration of this type of absorption very highly depends on the partial pressure of the absorbent in the gas phase [27]. In a chemical absorption process, the gas phase that is dissolved reacts with a component of the liquid phase. This process lies in the absorbent that has proved to be able to remove CO_2 from several gas mixtures, among them natural gas, synthesis gas, and various refinery streams [15].

2.4.1. Solvent for carbon dioxide absorption process

Since the key point of the chemical absorption process lies in the absorbent we can choose the cost-effective solvent with high-performance, high CO_2 loading capacity, low regeneration energy, and High gas solubility [2]. Some of the good solvents are aqueous solutions of alkanolamines, including Mono-ethanolamine (MEA) [9], di-ethanolamine (DEA) [11], tri-ethanolamine (TEA), and N-methyl di-ethanolamine (MDEA) [12], amino acid salts [28], sodium hydroxide [18], and aqueous solutions of ammonia [15].

2.4.2. Absorption into aqueous ammonia solution

With the mentioned drawbacks of normal alkanolamines, the search for a new and better solvent is still a very open and interesting question. Lately, aqueous solutions of NH_3 seem to be alternative solvents for removing CO_2 from flue gases [15]. Besides the general advantages such as high absorption efficiency [16], high absorption capacity [17], the low energy requirement for absorbent regeneration [1], and wide distribution of resources, aqueous ammonia could simultaneously remove SO_2, NO_x, and oxidized mercury [2, 16]. Furthermore, the by-products, amine salts produced during the reaction of ammonia with CO_2, SO_2, and NO_x, can be used as fertilizer for soil improvement [2].

2.4.3. Reaction mechanism of ammonia with carbon dioxide

When CO_2 encounters aqueous ammonia, reaction between the two mainly occurs in the liquid phase of the gas-liquid interface [1]. Generally, the reaction mechanism between aqueous ammonia and carbon dioxide is available in different literatures [1, 2, 7, 28]. The reaction in the

liquid phase of the CO_2-ammonia system which is reversible and very complicated is given as follows;

$$CO_2(g) + 2NH_3(aq) \rightarrow NH_2COONH_4(aq) \quad (2.1)$$

$$CO_2(g) + 2NH_3(l) + H_2O(l) \leftrightarrow (NH_4)_2CO_3(aq) \quad (2.2)$$

$$CO_2(g) + NH_3(l) + H_2O(l) \leftrightarrow NH_4HCO_3(aq) \quad (2.3)$$

The reactions (2.2) and (2.3) are reversible, with ammonium carbonate $(NH_4)_2CO_3(aq)$ or bicarbonate $NH_4HCO_3(aq)$ as the main products. The forward reactions are dominant at room temperature. While, the backward reactions occur at temperatures of around 38-60℃ [29].

Reaction (2.1) is composed of the following two steps.

$$CO_2(g) + NH_3(aq) \rightarrow NH_2COOH(aq) \quad (2.4)$$

This reaction is very fast and irreversible, and the reaction between aqueous ammonia and carbon dioxide is mainly controlled by the above reaction (2.4), which is a second-order reaction with first- order for CO_2 and NH_3respectively.

$$NH_3(aq) + NH_2COOH(aq) \leftrightarrow NH_4^+(aq) + NH_2COO^{-1}(aq) \quad (2.5)$$

The reaction (2.5) is then, $NH_2COONH_4(aq)$ hydrolyzes in solution instantaneous and generates free ammonia:

$$NH_2COO^{-1}(aq) + H_2O(l) \leftrightarrow HCO_3(aq) + NH_3(aq) \quad (2.6)$$

$$NH_3(aq) + H_2O(l) \leftrightarrow NH_3H_2O(aq) \quad (2.7)$$

The reaction (2.6) is too slow to influence the rate of the absorption directly. Aqueous ammonia is a weak alkali solution thus, the hydration of CO_2 in aqueous solutions would occur in the liquid phase, the reactions are as follows:

$$CO_2 + H_2O \leftrightarrow HCO_3^- + H^+ \quad (2.8)$$

$$CO_2 + OH^- \leftrightarrow HCO_3^- \quad (2.9)$$

The reaction rate for CO_2 absorption into ammonia solution mainly controlled by the reactions are given in Eq. (2.4) and Eq. (2.9) which can be described as follows.

$$r_{CO_2-NH_3} = k_2[NH_3][CO_2] \quad (2.10)$$

$$r_{CO_2-OH} = k_{OH}[OH^-][CO_2] \quad (2.11)$$

The overall reaction rate can be described as:

$$r = r_{CO_2-NH_3} + r_{CO_2-OH} = k_2[NH_3][CO_2] + k_{OH}[OH^-][CO_2] \quad (2.12)$$

The kinetic rate constant k_{OH} can be described in terms of temperature.

$$\lg(k_{OH}) = 13.635 - \frac{2895}{T} \quad (2.13)$$

2.4.4. Absorption into Alkanolamines

Alkanolamine is a term that is used for a chemical compound that has the structure include primary, secondary, ternary amines containing at least one OH and amine groups such as mono-ethanolamine (MEA), di-ethanolamine (DEA), and N-methyl di-ethanolamine (MDEA) [27]. The reactivity of amines to CO_2 follows the order of primary, secondary, and ternary amines. That is the primary amines have higher reactivity with CO_2 compared to secondary and tertiary amines and secondary amines have higher reactivity than tertiary amines towards CO_2 gases [27].

2.4.5. Reaction mechanism of Alkanolamine with carbon dioxide

As shown in the result of past works of literatures (27, 30) the reactions between CO_2 and MEA solution have been described by two mechanisms. Namely the zwitterion mechanism and the termolecular mechanism. The zwitterion mechanism consists of the formation of a complex called a zwitterion, followed by the deprotonation of the zwitterion by a base. All the species in the reaction are represented in an aqueous solution as follows.

Ionization of water:

$$2H_2O \overset{k_1}{\leftrightarrow} OH^- + H_3O^+ \tag{2.14}$$

Dissociation of dissolved CO_2 through carbonic acid:

$$CO_2 + 2H_2O \overset{K_2}{\leftrightarrow} HCO^- + H_3O^+ \tag{2.15}$$

Dissociation of bicarbonate:

$$HCO^- + H_2O \overset{k_3}{\leftrightarrow} CO_3^{2-} + H_3O^+ \tag{2.16}$$

Zwitterion formation from MEA and CO_2 reaction:

$$CO_2 + RNH_2 \overset{k_4 k_{-4} k_4}{\longleftrightarrow} RNH_2{}^+COO^- \tag{2.17}$$

Carbamate formation by deprotonation of the zwitterion:

$$RNH_2{}^+COO^- + RNH_2 \overset{k_5 k_{-5} k_5}{\longleftrightarrow} RNH_3^+ + RNHCOO^- \tag{2.18}$$

$$RNH_2{}^+COO^- + H_2O \overset{k_6 k_{-6} k_6}{\longleftrightarrow} H_3O^+ + RNHCOO^- \tag{2.19}$$

$$RNH_2{}^+COO^- + OH^- \overset{k_7 k_{-7} k_7}{\longleftrightarrow} H_2O + RNHCOO^- \tag{2.20}$$

Carbamate reversion to bicarbonate (hydrolysis reaction):

$$RNHCOO^- + H_2O \overset{k_8 k_{-8} k_8}{\longleftrightarrow} RNH_2 + HCO_3^- \tag{2.21}$$

Dissociation of protonated MEA:

$$RNH_3^+ + H_2O \overset{k_9 k_{-9} k_9}{\longleftrightarrow} RNH_2 + H_3O^+ \tag{2.22}$$

Bicarbonate formation:

$$CO_2 + HO^- \overset{k_{10} k_{-10} k_{10}}{\longleftrightarrow} HCO_3^- \tag{2.23}$$

Additional reactions become essential due to the significant contributions of bicarbonates and carbonates in the aqueous solutions.

$$RNH_2{}^+COO^- + HCO_3^- \overset{k_{11}k_{-11}k_{11}}{\longleftrightarrow} H_2CO_3 + RNHCOO^- \quad (2.24)$$

$$RNH_2{}^+COO^- + CO_3^{2-} \overset{k_{12}k_{-12}k_{12}}{\longleftrightarrow} HCO_3^- + RNHCOO^- \quad (2.25)$$

These additional reaction equations 2.24 and 2.25 are essential in describing the zwitterions mechanism [30]. Based on this reaction scheme, the general rate of reaction of CO_2 with MEA via the zwitterion mechanism could be described as

$$r_{CO_2-MEA} = \frac{[CO_2][RNH_2] - {}^{k_{-4}}/_{k_4}[RNHCOO^-](\frac{\sum K_{-b}[BH^+]}{\sum K_b[B]})}{\frac{1}{k_4} + \frac{k_{-4}}{k_4 \sum K_b[B]}} \quad (2.26)$$

Where B designates any species in the solution that can deprotonate the zwitterions intermediate into carbamate [30].

The termolecular mechanism assumes that the reaction between CO_2 and MEA is of a single-step. The forward reaction rate for this mechanism given as

$$r_{CO_2-MEA} = -\left(K_{RNH_2}[RNH_2] + K_{H_2O}[H_2O]\right)[RNH_2][CO_2] \quad (2.27)$$

2.4.6. Absorption into Sodium Hydroxide

NaOH solution is another alternative absorbent for CO_2 absorption. The absorption mechanism of CO_2 into NaOH aqueous solution is explained as follows [18]. First, Na+ and OH^- are completely ionized in pure water because NaOH is a very strong alkaline. Secondly, when gaseous CO_2 is fed into the NaOH solution to be absorbed, CO_2 is physical to aqueous CO_2, as in the following equation

$$CO_2(g) \rightarrow CO_2(aq) \quad (2.28)$$

Then aqueous CO_2 react with OH^- to generate HCO_3^- and CO_3^{2-} as expressed in the following equation.

$$CO_2(aq) + OH^-(aq) \leftrightarrow HCO_3^-(aq) \quad (2.29)$$

$$HCO_3^-(aq) + OH^-(aq) \leftrightarrow H_2O(l) + CO_3^{2-}(aq) \quad (2.30)$$

The overall reaction between CO_2 and NaOH solution can be expressed as:

$$CO_2(aq) + 2OH^-(aq) \leftrightarrow H_2O(l) + CO_3^{2-}(aq) \quad (2.31)$$

This reaction is second order and may be considered to be an irreversible reaction.

2.5. Bubble Column reactor

Bubble column reactors are an apparatus that belongs to the general class of multiphase reactors that are widely used in petrochemical, biochemical, and metallurgical processes to carry out gas-liquid or gas-solid-liquid reactions [20, 21]. These apparatus are presented in the most simple form basically in vertically square [31] and cylindrical [20]. The absence of moving parts, their low operating and maintenance costs, and the excellent mass and heat transfer rates explain the large number of applications developed with this kind of reactor against the others [18, 19]. In their operation, the gas normally aerated or sparged in form of bubbles into the liquid phase through the gas distributor located at bottom of the column reactor [18, 19]. With a certain velocity, it will be dispersed by the distributor into a bubble to the continuous liquid phase to produce the dynamic turbulent stream that causes the optimum gas exchange.

In general, there are semi-batch and continuous modes of operation for bubble columns reactor [32]. In the first mode, semi-batch operation [32], the liquid is in the batch that stays in the bubble column while the gas phase is continuously fed at a particular superficial gas velocity, through the liquid phase [29, 31]. In continuous modes of operation, however, the continuous phase enters a superficial liquid velocity in which a superficial liquid velocity is less than superficial gas velocity [19].

2.5.1. Design of a bubble column reactor

The design of the bubble column reactor is based on the variation of parameters from an existing design. There are only minor redesign efforts involved in the improvement of an existing bubble column reactor [22]. A successful design of bubble column reactors generally depends on the quantification of three main phenomena: (i) heat and mass transfer characteristics; (ii) mixing characteristics; (iii) chemical kinetics of the reacting system [19]. More specifically, to design bubble column reactors, the following key factors such as gas hold-up, volumetric mass transfer

coefficient, specific interfacial area, bubble size, and kinetic rate constants, are fundamental for the proper design and the operational control of gas-liquid reactors [18, 19].

2.5.2. Fluid dynamics and regime analysis in bubble column

The characterization of hydrodynamic in bubble column reactors has a significant effect on the operation and performance of bubble columns [18, 19]. This hydrodynamic is strongly dependent on the flow regime in which it is operating [18, 32]. According to the superficial gas velocity employed in the column, there are three types of flow regimes that are commonly observed in bubble columns which are the homogeneous (bubbly flow) regime, the heterogeneous (churn-turbulent) regime, and the slug flow regime [19].

The homogeneous flow regime is obtained at low superficial gas velocities, approximately less than 5 cm/s in semi-batch columns [18, 32]. This flow regime is characterized by a homogeneous gas bubbles distribution, weak interactions among gas bubbles and between gas and liquid phases, almost constant gas bubbles residence time, sharp unimodal size distribution of the gas bubbles, and almost no liquid back-mixing. The heterogeneous regime is maintained at higher superficial gas velocities (greater than 5 cm/s in batch columns). This regime is characterized by strong gas-liquid mixing and optimal mass/heat transfer because large and fast-rising gas bubbles induce strong circulations and create back-mixing or re-circulation zones wherein the small gas bubbles are entrained [18,32].

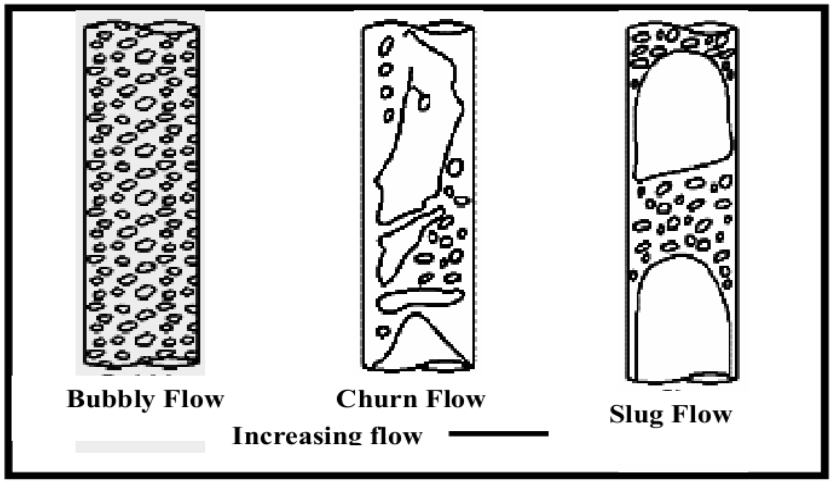

Figure 2.1: Schematic of possible flow regimes in bubble columns [19].

A slug flow regime has been only observed in small diameter (≤ 0.0015 cm) laboratory columns at high gas flow rates that exhibit very poor mixing and mass transfer. [34]. The transition from one flow to another flow is characterized by the formation of local liquid recirculation patterns in the reactor created by the increasing population of large gas bubbles [19]. One of the most efficient ways of characterizing the possible regime boundaries of a bubble column system is through the use of flow regime maps [35]. As shown in figure (2.2) this map shows the influence of both column diameter and superficial gas velocity on regime transition.

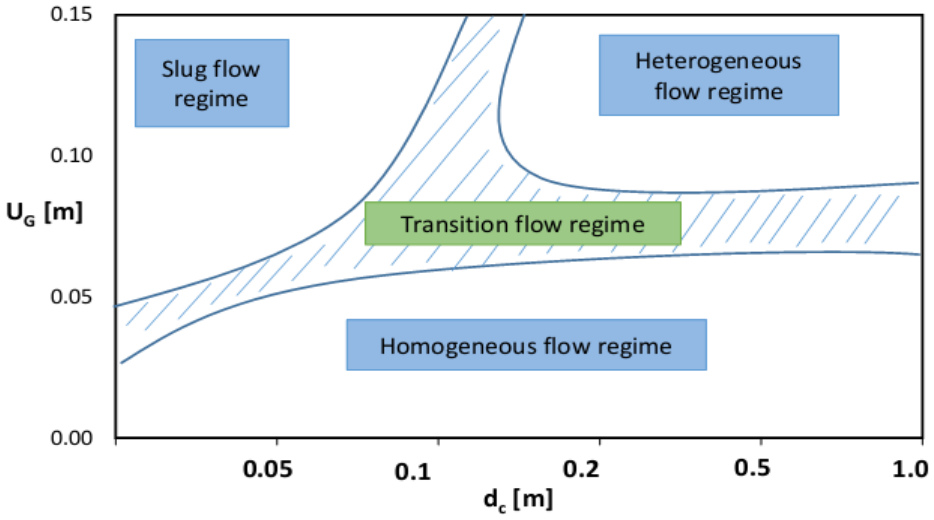

Figure 2.2: Flow regime map for bubble columns [19].

2.5.3. Gas Holdup in Bubble Columns

The gas holdup is dimensionless key parameters that play an important role in the design performance and characterizing of transport phenomena in the bubble column [19]. It is defined as the volume fraction of the gas phase occupied by the gas bubbles within a bubble column at any point during its operation [32]. Gas holdup depends predominantly on the diameter of the gas bubbles and their rising velocity. That means the gas holdup is high when the number of bubbles is high and their diameter small [36].

There are different methods available to measure gas holdup such as pressure change, volume expansion, and flow isolating technique. Among those methods, the easiest and usual way is the

measurement of the differential pressure between two points in the column [18, 35]. The relation is given as

$$\varepsilon = (\frac{\rho_L}{\rho_L - \rho_G})(1 - \frac{\Delta P}{\rho_L g \Delta H}) \quad (2.32)$$

Where ε is gas holdup, ρ is density, ΔP is pressure drop, g is gravitational acceleration and ΔH is height difference. The subscript L and G indicates the liquid and gas phase respectively.

Based on the method of volume expansion the overall gas holdup was calculated as the following equation [36, 37].

$$\varepsilon = \frac{\Delta L}{\Delta L + L} \quad (2.33)$$

Where L is the initial liquid level and ΔL is the level expansion after gas dispersion.

2.5.4. Bubble definition and its characteristics

Bubble technology is expected to be a cost-effective and environmentally friendly technology with great potential in many applications such as particle separation, disinfection, organic-matter reduction, and water treatment [38, 39]. This is because bubbles have the ability to high mass transfer efficiency, relatively lower rising velocity, easily tailored surface charge, free radical generation ability, and improved collision efficiency. Many researchers can be categorizing the bubble as a micro-bubble, fine bubble, and ultrafine bubble with a different size range. [40] summarize the size categories of different bubbles with their major properties as shown in figure (2.3).

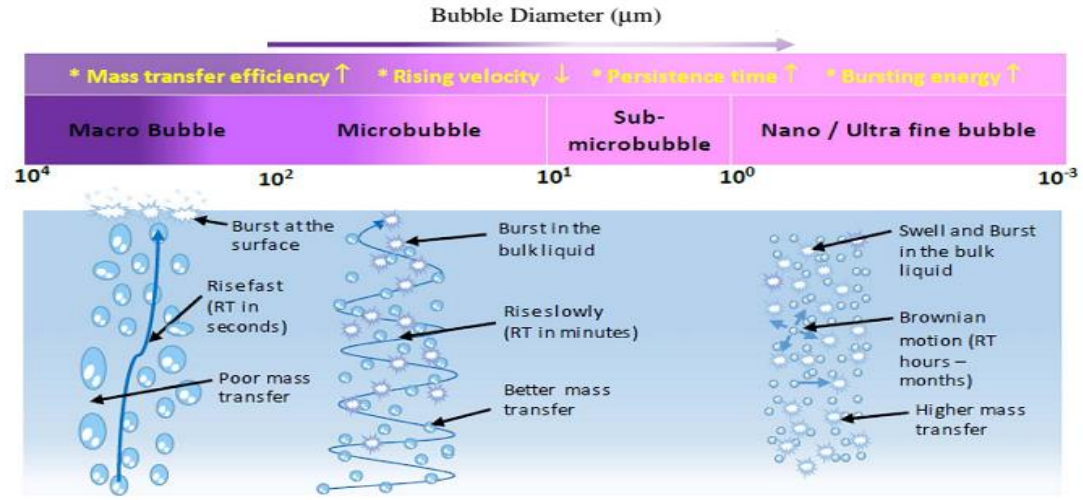

Figure 2.3: Different range of the bubble size and major properties [40].

The knowledge of the bubble size distribution in BCRs is important because they define bubble rise velocity and holdup. The size of the gas bubbles presents combined with the gas holdup will determine how much interfacial area is available for the transfer of the gaseous species to and from the liquid-phase [42].

2.5.4.1. Bubble Generation

An appropriate method of bubble generation is another key to meet the different applications of bubbles mentioned above. The overall process of bubble formation, growth, and the collapse of macro-bubble is often referred to as cavitation [38, 41]. Different studies can be classified cavitation based on the mode of operation into four categories i.e. Hydrodynamic cavitation, acoustic or sonication, Electrochemical cavitation, and Mechanical agitation. In all methods, cavitation is generated based on the reduction of pressure using surface tension and energy deposit [40]. Hydrodynamic cavitation is the most frequently used in industrial applications because of low energy consumption and widely applicable to various application environments [41]. Its pressures variation was achieved by a flowing fluid causing a velocity variation and applying an acoustic field and some of the typical bubble generators are spiral liquid flow type, pressurized dissolution type, ejector type, and venture type [38, 39]. The pressure is reduced below its vapor pressure in all systems because of the high velocity inside the flow path [40].

2.5.4.2. Bubble Measuring Technique

Accurate measurement of bubble size is important to estimate the gas holdup, mass transfer rate, and gas dispersion [44]. Several techniques have been developed that are used for measuring bubble size and their distribution [40]. Among these the most typically used are the laser-diffraction particle-size analyzer, atomic force microscope, and image analysis. The image analysis method is perhaps the most commonly used technique for measuring bubble size by taking an image using a digital camera [44]. This technique can be used for measuring both the size of the bubble and the shape of the projection of the bubble [44] and the minimum bubble size of 0.8 μm [40]. The laser-diffraction particle-size analyzer measurement is based on their light-scattering properties and is used to obtain the average size of a large number of a bubble without a visible image [40].

2.5.5. Mass transfer properties

The mass transfer between gas and Liquid within a bubble column reactor is another criterion for critical design and scale-up. The rate mass transfer from a gas-to-liquid phase in bubble column often controls the process efficiency that depends on the size distribution of the bubbles, the rising velocity of the bubbles, surface area to volume ratio, coalescence and breakup, gas-liquid hydrodynamics, phase mixing, and physical properties [38, 43]. Based on the two-film theory the rate of mass transfer in BCR depends on the gas and liquid phase mass-transfer coefficient, the specific interfacial area, and the concentration gradient between the two phases [40].

2.5.6. Volumetric Gas-Liquid Mass Transfer Coefficients

For gas-liquid systems, the overall mass transfer rate per unit volume of the dispersion in a bubble column is governed by the liquid side mass transfer coefficient [18, 29] assuming that the gas side resistance is negligible. Its variability is controlled by the interfacial area between the discrete bubble phase and the continuous liquid phase [13, 44]. For the absorption purpose, there are two kinds of absorption methods which are physical and chemical treatments depending on the absorbents [11]. In physical type, the mass transfer flux can be quantified as the product of the overall mass transfer coefficient $K_l a$ and the difference in concentration between the saturated concentration C_A* and the concentration of the species of interest in the continuous liquid phase C_A, [29, 36] such that:

$$N_{\mathrm{A}} = K_l a(C_{\mathrm{A}^*} - C_{\mathrm{A}}) \tag{2.34}$$

For chemical absorption, the mass transfer flux is the consequence of chemical reactions on the mass transfer is done using enhancement factor (E) [39].

$$N_{\mathrm{A}} = E * K_l a(C_{\mathrm{A}^*} - C_{\mathrm{A}}) \tag{2.35}$$

As discussed in the literature of [36, 37,38 44] the overall mass transfer coefficient is given as the product of the liquid side mass transfer coefficient (K_l) and the specific interfacial area (a). These two parameters can be evaluated separately [38]. The specific interfacial area can be defined as the bubble surface area in a gas-liquid dispersion and commonly calculated from the bubble Sauter mean diameter d_s and the gas holdup ε_g using the following equation:

$$\alpha_s = \frac{6\varepsilon_g}{d_s} \tag{2.36}$$

In another way, the overall mass transfer coefficient of carbon dioxide is calculated without separating the liquid-side mass transfer coefficient (K_l) and the specific interfacial area (a) from a mole fraction of carbon dioxide and inlet flow rate [1].

$$K_l a = \frac{Q}{PH}[\ln\frac{y_1}{y_2} + (y_1 - y_2) \tag{2.37}$$

Where Q is inlet gas flow rate, H is the height of the column, y_1 and y_2 are the mole fraction ratios of CO_2 to gas-phase entering and leaving the absorption column, respectively.

The enhancement factor is a function of components concentration and type of reaction in a process that can be larger or equal to one. It is the ratio of the mass flux with a chemical reaction to the mass flux without chemical reaction [47].

$$E = \frac{N_{\mathrm{A}}}{K_l a(C_{\mathrm{A}^*} - C_{\mathrm{A}})} \tag{2.38}$$

2.6. Previous work on CO_2 absorption technology in bubble column reactor

Zhao et al., 2013 studied the effect of reactor geometry on ammonia-based CO_2 capture performance. The authors used a series of bubble column reactors with a bubble size of 1.5 mm and the same volume of working liquid but varied geometry (liquid height-to-diameter ratios H/D = 0.93, 2.04, and 3.98) as shown in figure (2.4). In their experiments, the reaction (operating) parameters including ammonia concentration (7-28 %w/w), CO_2 inlet concentration (10-15 %v/v), and total flue gas flow rate (1-2.5 L/min) and reaction temperature (10-40℃) were systematically varied to examine their effects on CO_2 capture efficiency at different reactor geometry.

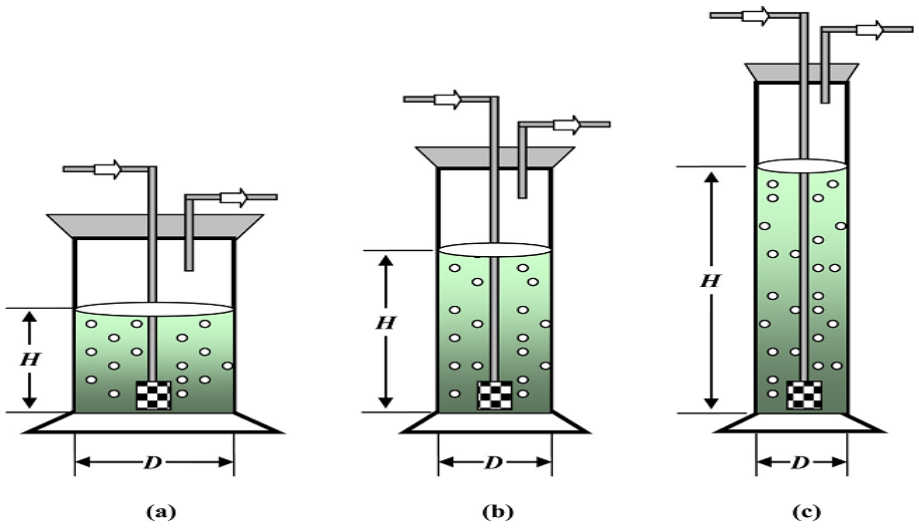

Figure 2.4: Bubble column reactors with varied geometry (aqueous ammonia work volume: 200 ml): (a) D = 65 mm and H = 60.3 mm with H/D = 0.93; (b) D = 50 mm and H = 101.9 mm with H/D = 2.04; (c) D = 40 mm and H = 159.2 mm with H/D = 3.98.

From this experiment, when reactors are operated at the ammonia concentration of 14%, the CO_2 inlet concentration of 15%, the flue gas flow rate of 1.5 l/min the reaction temperature of 20℃, and the operating time of 1200se (20 min), the result shows that CO_2 capture efficiencies were 98.89% for H/D = 3.98, 97.69% for H/D = 2.04 and 93.11% for H/D = 0.93, respectively [2]. When the ammonia concentrations varied from 7% to 28% w/w the maximum CO_2 capture efficiency increased from 97.18% to 100% for H/D = 3.98, 93.11–99.89% for H/D = 2.04 and 90.75–97.69% for H/D = 0.93, respectively. This is because of the ammonia-CO_2 chemical reaction kinetics and the classic two-film theory, high aqueous ammonia concentration enhancing

the mass transfer and the forward reaction on the liquid side, leading to the increase of CO_2 capture efficiency [2].

When the CO_2 inlet concentration increased from10% to 20% v/v the maximum CO_2 capture efficiency decrease from 99.09% to 98.39% for H/D = 3.98, 98.19–97.18% for H/D = 2.04 and 96.38–91.41% for H/D = 0.93, respectively. This is because increasing CO_2 inlet concentration is simultaneously equivalent to reducing the molar ratio of NH_3 to CO_2 causing the decrease of CO_2 capture efficiency. Since the flue gas flow rate increase the CO_2 to NH_3 molar ratio the maximum CO_2 capture efficiencies decreased from 99.89% to 98.29% for H/D = 3.98, 98.29–96.57% for H/D = 2.04 and 97.18–92.50% for H/D = 0.93 when gas flow rate is varied from 1 to 2.5 L/min. The reaction temperature has also direct relation with CO_2 capture efficiencies that mean when reaction temperature varied from 10℃ to 40℃ the maximum CO_2 capture efficiencies increased from 97.43% to 99.40% for H/D = 3.98, 96.57–98.89% for H/D = 2.04, and 91.37–97.18% for H/D = 0.93. Generally as concluded by [1] the CO_2 capture efficiency for all three reactors increased with increasing the ammonia concentration and the reaction temperature (below 40℃) while decreasing with increasing CO_2 inlet concentration and gas flow rate.

Pashaei et al., 2017 studied solubility, and the chemical absorption rate of carbon dioxide into aqueous solutions of di-ethanolamine (DEA) in a stirred bubble column reactor. In this work, they also examine the effects of stirrer speed, amine concentration, CO_2 partial pressure, and CO_2 loading on absorption rate and solubility by using the experimental conditions of, amine concentration in the range of 0.2–2.0 M, CO_2 partial pressures in the range of 2.4–3.6 kPa, stirrer speed in the range of 0–600 rpm, CO_2 loading in the range of 0.1–0.7mole of CO_2 per mole of amine. Their results showed that mass transfer flux and absorption percent of CO_2 were varied in the range of 34–59% and 0.35–4.32 kmolm−2 s−1, respectively. Again it shows CO_2 absorption rates into an aqueous solution of DEA were increased with an increase in stirring speed because the holdup increases due to less bubble diameter.

The CO_2 partial pressure increases as the mass transfer flux of CO_2 increases and this is obvious because the increase in the partial pressure of CO_2 in the gas phase leads to an increase in the driving force of mass transfer. Also, the mass transfer coefficient decreases with the CO_2 partial

pressure increases, at DEA concentration. This is because the influence of DEA concentration on the absorption rate is very fast when the conversion of DEA concentration is higher.

Bentes et al., 2015 studied the CO_2 absorption process in aqueous solutions of 3-amino-1- propanol using a bubble column reactor (BCR). This study is focused on the absorption rate, reactor hydrodynamics, and the changes in the liquid phase temperature. The absorption rate study data on this work is obtained by monitoring the inlet and outlet gas flow rate in the gas-liquid contactor. The result showed an increase in amine concentration increases the time needed for the absorption rate to reach saturation. For the lower amine concentration solution, this period is very short and the absorption rate reaching saturation in a shorter time.

Also, the reactor hydrodynamics in this work is based on the analysis of gas holdup, bubble size distribution, and gas-liquid interfacial area under different experimental conditions. The result shows that there is an increase in gas-liquid interfacial area with time because at the beginning of the experiments, a high concentration of amine is available to react with carbon dioxide and this causes the great decrease of bubble size during the rise in the liquid phase takes place. This fact produces a high decrease in a gas hold-up and the interfacial area. Another result shows that when amine concentration is higher in the liquid bulk, it produced an increase in the interfacial area. This is due to the surface tension decrease and because a small bubble formed.

Chu et al., 2017 studied CO_2 absorption in the bubble column using an ammonia solution. In this study the effects of the orifice size and number, and the operating conditions of gas flow rate and operating pressure, on the mass transfer and input energy of the BCR are investigated. 13 BCRs with different geometries are simulated under various working conditions as shown table (2.2) below.

Table 2.2: Detail information of the bubble column reactor used by Chu et al., 2017.

No	H(mm)	D(mm)	H/D	Orifice Size (mm)	Orifice number	Orifice position
Ao	*180*	60	3	4	1	Bottom
A1	180	60	3	6	1	Bottom

A2	180	60	3	8	1	Bottom
A3	180	60	3	10	1	Bottom
A4	180	60	3	4	2	Bottom
A5	180	60	3	4	3	Bottom
A6	*180*	60	3	4	4	Bottom
A7	180	60	3	**2**	4	Bottom
B	150.8	65	2.32	4	1	Bottom
C	113.2	75	1.51	4	1	Bottom
D	78.6	90	0.87	4	1	Bottom
E	226.8	53	4.28	4	1	Bottom
F	276.4	48	5.67	4	1	Bottom

As discussed by Chu et al., 2017 the mass transfer process inside the BCR is influenced by the bubble size, which is governed by the orifice size and the orifice number of the gas sparger. Four BCRs (A0, A1, A2, and A3) with different orifice sizes but the same height-to-diameter ratio are investigated under the working condition CO_2 mole ratio in gas phase entering BCR (20%), gas flow rate (6m/min/m^2), NH_3 concentration (4kmol/m^3), the volume of the solvent in BCR (0.5 L). The result shows the CO_2 capture efficiency decreases with increasing the orifice size because the orifice size can influence the size of the bubble and then affect the interfacial area as well as the gas hold up. The increased orifice size can improve the volumetric overall mass transfer coefficient of CO_2 absorption and increase the CO_2 flow rate, which is beneficial to the mass transfer.

Five BCRs (A0, A4, A5, A6, and A7) with different orifice numbers are investigated under the same working condition. The result shows that the CO_2 capture efficiency and the gas hold-up increase with increasing the orifice number and decreases with increasing the orifice size. The increased orifice number can improve the volumetric overall mass transfer coefficient of CO_2 absorption by increasing the CO_2 flow rate. They also investigate the effect of the height-to-diameter ratio by considering Six BCRs (A0, B, C, D, E, and F) at different height-to-diameter ratios. They obtained the result that the CO_2 removal efficiency and volumetric overall mass transfer coefficient of CO_2 absorption increase with increasing the height-to-diameter ratio. As a

consequence, it is essential to take the height-to-diameter ratio into account for the design of BCR, and they recommended a height-to-diameter ratio of 5.76 to meet the demands of both mass transfer and energy conservation.

They also examine by varying the ammonia concentration from 4 to 8mole/m^3 and CO_2 mole ratio in the gas phase entering BCR from 10 to 20%. They obtained the CO_2 removal efficiency and volumetric overall mass transfer coefficient of CO_2 absorption decrease as the inlet CO_2 molar fraction increases, and increase as the ammonia concentration increases, this is because the increased ammonia concentration results in a higher reaction enhancement factor, thus accelerate the reaction rate.

CHAPTER THREE

MATERIALS AND METHODS

This chapter aims to present the materials required, the design procedure of a bubble column reactor, and proper experimental techniques that need to be followed for various experiments that will be performed in this thesis work. For convenience, design procedure, and experimental techniques are categorized into three sections. The first section describes the designing of the bubble column reactor as well as the designing of the venturi based splitter micro-bubble generator. The second section describes the manufacturing of the column and bubble generator and the last section describes the experimental on CO_2 absorption using different solvents by applying micro-bubble assisted system and conventional bubble assisted system.

3.1. Materials

In this work, aqueous ammonia solution, sodium hydroxide, and mono-ethanolamine solutions were used as an absorbent for the removal of CO_2. Tap water was also used to prepare the solution with different concentrations (1%, 3%, 5%, and 7%V/V), that were used to remove the CO_2 for this experimental research. A gas phase of CO_2 with 100% purity was feed into a gas-liquid reactor via venturi type air liquid mixer. Afterwards, exhaust gas analyzer (Infralyt smart CT 159.02) and, digital microscope was used to measure the amount of CO_2 at the outlet of the column and to analyze the image of micro-bubble generated respectively.

3.2. Research Methodology

The following methodology in Figure (3.1) was followed during this research work.

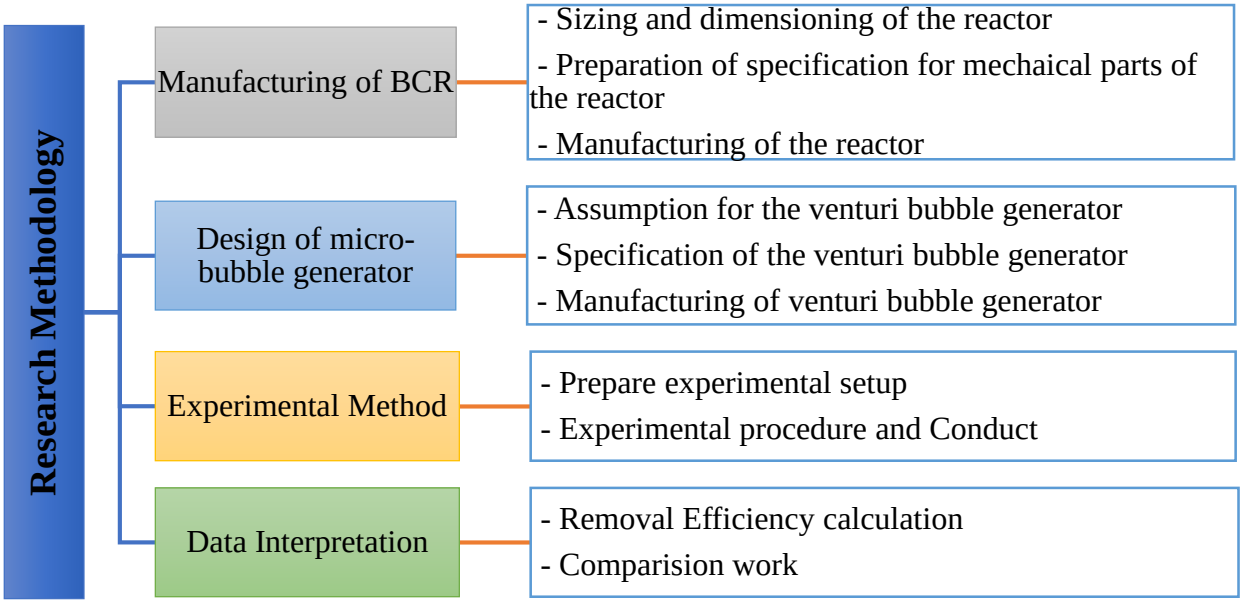

Figure 3.1: Research Methodology.

3.3. Design of a bubble column reactor

The main goal of the designs of the bubble column reactor in this work is to test CO_2 absorption efficiency using solvent and fine/micro-bubbles. For this purpose, it is necessary to develop a bubble column that consists of a modern acrylic glass column material for fluid visualization, a stable column with a well-built frame holder, easy to handle and transport, cost-effective material, and easy to clean, service, and maintenance.

For the design purpose, the following assumption were made: -

- ✓ A reactor is normally operated at a steady-state,
- ✓ Pressure drop along the reactor is negligible,
- ✓ Well mixed or spatial variation in concentration, temperature, or reaction rate throughout the column is constant.

Since the reactor designed was based on the assumption of a well-mixed flow type a CSTR design equation was used as shown in Appendix A. This assumption was validated using residence time

distribution (RTD) by sodium chloride step experiment and calculation of reactor dispersion number $\frac{D}{UL}$ or inverse pellet number, which is a dimensionless number and a parameter that measures the extent of axial dispersion as discussed by Octave Levenspiel [48]. Thus, $\frac{D}{UL} \rightarrow 0$ negligible dispersion, hence plug flow, $\frac{D}{UL} \rightarrow \infty$ large dispersion hence mixed flow and $\frac{D}{UL} > 0.01$ large deviation from plug flow. This dispersion number is evaluated by measuring the meantime of passage (ṫ), which represents when the curve passes by the exit and variance (σ^2), which represents the square of the spread of the distribution as it passes the column exit and has units of (time)^2. These measures, ṫ, and σ^2, are directly linked by theory $\frac{D}{UL}$, as shown in Appendix B.

3.3.1. Specifications of the bubble column reactor

The bubble column reactor designed for CO_2 absorption, in this work is rectangular and was made from a modern acrylic glass which has a square cross-section (W x L) of 0.1 x 0.1 m^2 and a height (H) of 1m. At the top of the column, the conical shape with a height (H) of 0.2m is also designed to sequestrate the CO_2 out of the column. Generally, the dimension of the reactor and general design specifications are summarized in table 3.1.

Table 3.1: Design specifications of the bubble column reactor.

Index	Value
Column Material	Modern acrylic glass
Height of the Column (mm)	1000
Height of the Cone (mm)	200
Cross section area column (WxL) (mm)	100x100
Wall thickness (mm)	6
The diameter of the Bottom glass (mm)	200
The diameter of injection Nozzle (mm)	1.5
Size of the bottom and top plate (mm)	400x400

3.3.2. Mechanical part of the bubble column reactor

The reactor has different mechanical parts such as the reactor (bubble column reactor), cone, top and bottom plate, frame, injection nozzle, venture type bubble generator, flow meter, pump, ball valves, non-returnable valve, and caster wheel as shown in Figure 3.2. These functions of these mechanical parts of the column are summarized in Table 3.2.

a. 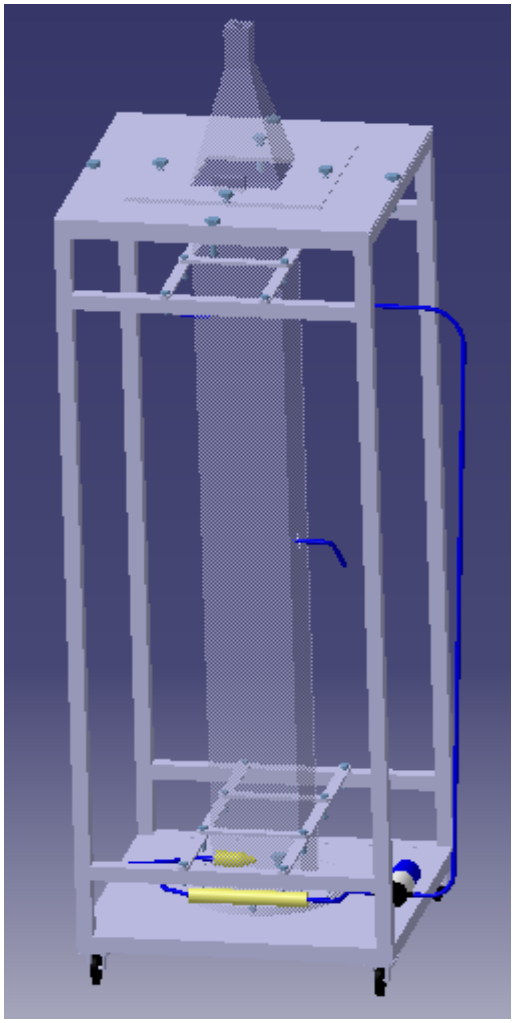 b. 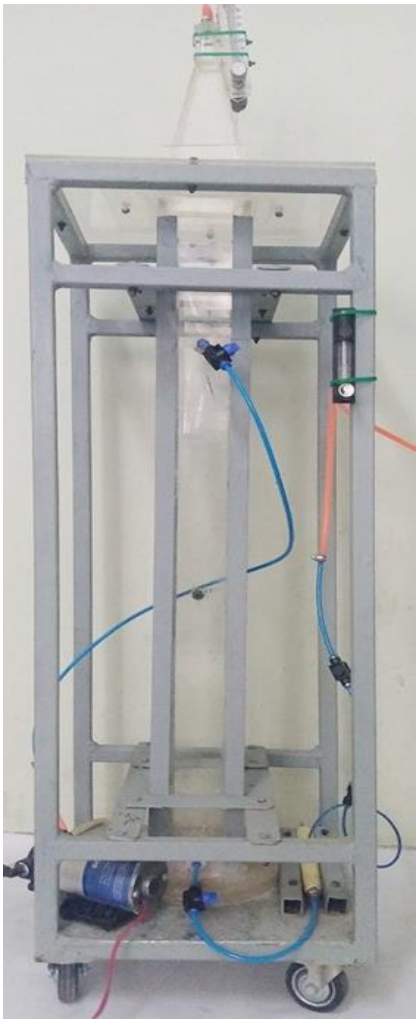

Figure 3.2: Bubble column reactor: (a) Drawing of bubble column reactor and (b) Manufactured bubble column reactor.

Table 3.2: Mechanical parts of the bubble column reactor and their functions.

Name of part	Part function
Metal profile	An easy to assemble framework to ensure column stability
Nozzle	To diffuse carbon dioxide micro-bubble to the column
Ball valve	Control liquid/gas flow through in/out of the column
Caster wheel	A steered wheel that serves as an absorbing shock and vibration
Flowmeter	Meter for measuring flow rate of gas
Top and bottom plate	To hold and support column weight and profile
Column	Contain and control gas-liquid reactions
Cone	To sequestrate the CO_2 at the outlet of the solvent
Air Diffusers	To diffuse carbon dioxide to the column
O-Ring	Elastomer sealing gasket to prevent liquid leakage
Pump	To recycling the solvent and pumping to the venture

3.4. Design of microbubble generator (venturi tube)

The bubble generator used for this work is venture type bubble generator that is used to mix carbon dioxide and solvent for the production of a carbon dioxide microbubble. In a venturi bubble generator, the gas is introduced at the throat by increasing the velocity and decreasing the pressure under inlet pressure. The tube has three sections such as converging, throat, and diverging section, and four geometrical parameters such as inlet angle, throat length, outlet angle, and diameter of the throat. When the velocity of liquid in the throttle, (at number 2 of Fig.3.3 (a)) increases, the pressure decrease helps the injection of carbon dioxide to the system with a low-pressure supply system. The geometry of the venturi tube is constructed from the Teflon bar by dividing it into five-part as shown in Figure 3.3.

a.

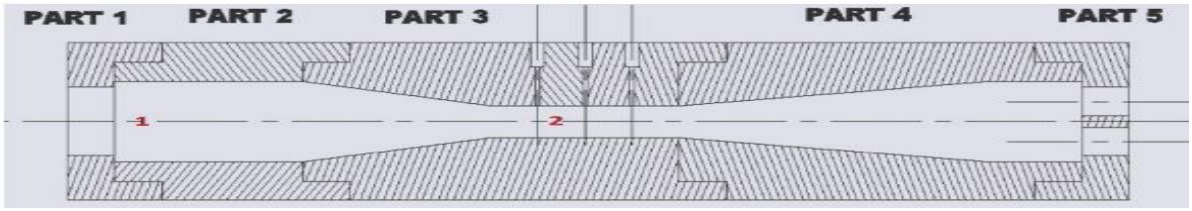

b.

b.

Figure 3.3: Venture tube: (a) drawing of venture tube and (b) manufactured venture tube.

The mathematical equation can be obtained by directly applying Bernoulli's theorem for a real fluid by dividing it into two sections. The first section is between the inlet and injector (section 1) and the start of the throat (Section 2), assuming a horizontal arrangement the equation becomes as follows: -

$$\frac{P_1}{\rho g} + \frac{V_1^2}{2g} + Z_1 = \frac{P_2}{\rho g} + \frac{V_2^2}{2g} + Z_2 \tag{3.1}$$

Where P_1 and P_2 are pressure, V_1 and V_2 are velocities, Z_1 and Z_2 are the elevations at section 1 and 2 respectively, ρ density of solution and g is gravity.

Since the pipeline is horizontal $Z_1 = Z_2$ the equation (3.1) may be given

$$P_1 + \frac{1}{2}V_1^2\rho + \rho g Z_1 = P_2 + \frac{1}{2}V_2^2\rho + \rho g Z_2 \tag{3.2}$$

By applying the continuity equations; $Q_1 = Q_2$

$$A_1 V_1 = A_2 V_2 \tag{3.3}$$

Rearranging equation of continuity and substituting in equation (3.2) gives

$$P_2 = P_1 + \frac{1}{2}V_1^2\rho(1 - (\frac{A_1}{A_2})^2) \quad (3.4)$$

Generally, the geometrical parameter that used for venture tube was calculated based on the assumption in appendix D and their value was summarized in table 3.3.

Table 3.3: Specification of geometrical parameters of venturi tube.

Parameters	Value
Diameter at inlet (D_1)	6mm
Diameter at the throat (D_2)	3mm
An area at the inlet (A_1)	$2.83*10^{-5}\ m^2$
Area at throat (A_2)	$0.7065*10^{-5}\ m^2$
Velocity at the inlet (V_1)	0.8834 m/s
Velocity at the throat (V_2)	3.5336 m/s
The pressure at the inlet (P_1)	1.29 atm
The pressure at the throat (P_2)	1.23 atm
The total length of the tube	160 mm
Inlet angle	4.29°
Outlet angle	2.23°

3.5. Experimental setup

Figure (3.4) shows the schematic diagram of the experimental setup used for this work. It consists of six parts including the bubble column reactor, CO_2 collection part, CO_2 supply system, venture type bubble generator, exhaust gas analyzer, and sampling port. The bubble column reactor is a rectangular shape that is made from acrylic glass with a specified area of $0.01m^2$. The height of the column from the nozzle inlet is 1m and the testing section height is 0.8m. On the top of the column, there is also a conical shape that has a similar surface area to the column and a height of 0.2m that was used to collect the outlet CO_2 from the solution. The volume of liquid-absorbent has

been set fixed and equal to 8L in all experiments, and the volume of the CO_2 collection part above the testing section is 2.69L.

The CO_2 was supplied from the cylinder and introduced into the venture bubble generator at the throat section by measuring its flow rate via a CO_2 flowmeter. The solution that was used as absorbent was introduced into the column at the top of the column through a batch process and recycled to the venturi bubble generator through a recirculation pump. The recycled solution was mixed with the CO_2 in the venturi at the throat section and introduced to the column reactor by a nozzle at the bottom of the column. An exhaust gas analyzer was used to measure the percentage volume of CO_2 sequestrated at a different time in the CO_2 collection part.

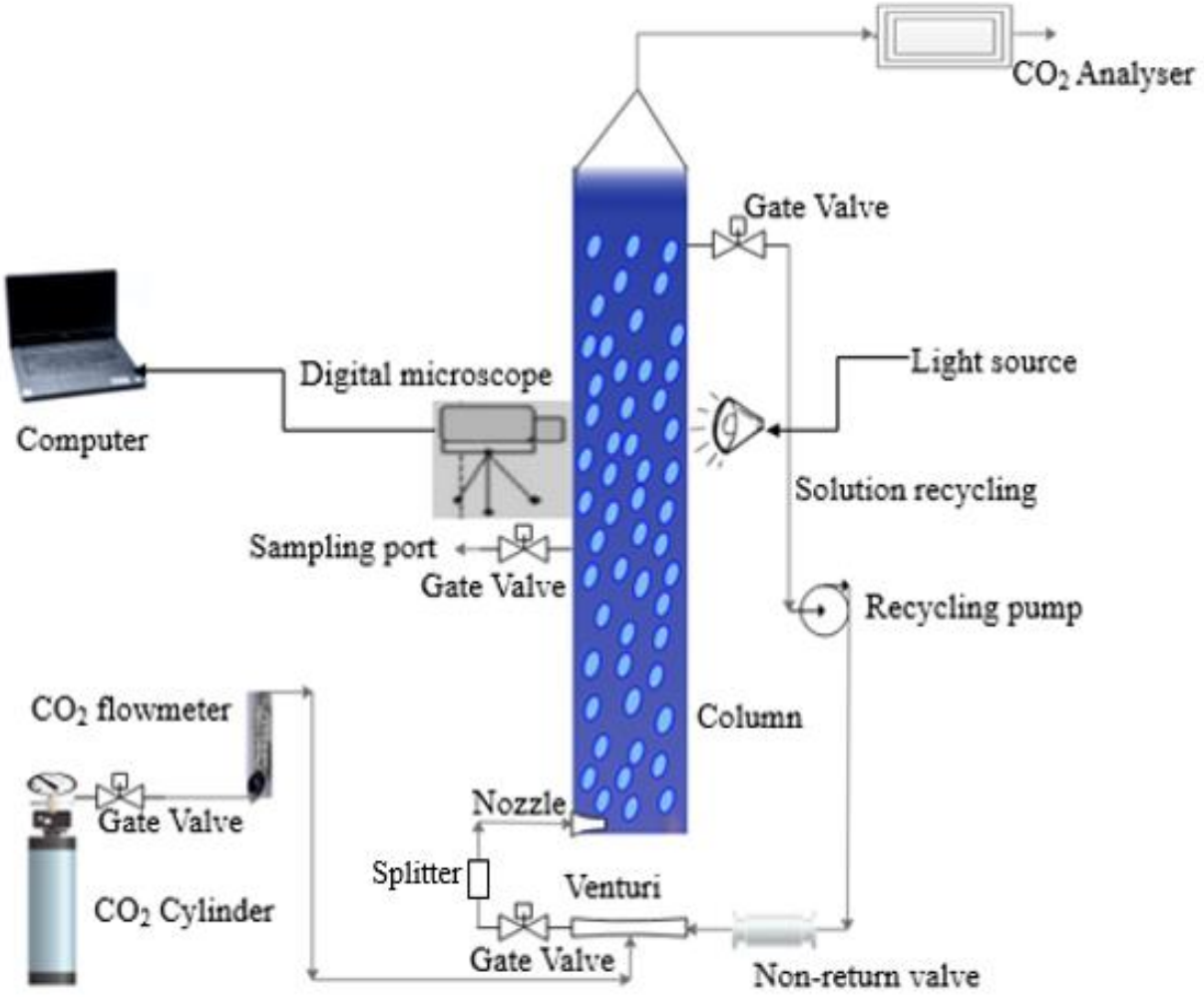

Figure 3.4: The Experimental setup.

3.6. Experimental procedure

The Ammonia, Sodium hydroxide and Mono-ethanolamine solution were prepared by different concentrations (1%, 3%,5%, and 7%) and introduced to the column. The CO_2 micro-bubble is generated in the venturi type splitter with the solvent and continuously introduced at the bottom of the column in contact with the liquid phase and rise to the top of the column. As the bubbles rise, interphase diffusion takes place and saturation point of equilibrium is achieved.

All experiments were carried out under room temperature and atmospheric pressure in the CO_2-solvent system. To analyze the bubble size, the sample was taken at the sampling port. The CO_2 concentration was measured at the outlet of the column by an exhaust gas analyzer. To investigate the effect of the CO_2 removal efficiency with different variables, the experiment was conducted at various solvent concentrations, CO_2 flow rate, and bubble size. Generally, the experimental condition used in this work is summarized in the Table 3.4.

Table 3.4: The experimental condition used in this work.

Index	Value
Height of testing solution (m)	0.8
The volume of the solution (L)	8
Solvent concentration (%V)	1, 3, 5 and 7
CO_2 concentration (%V)	100
CO_2 flow rate (L/min)	1,1.5, 2,and 2.5
Pressure	Atmospheric pressure

3.7. Carbon dioxide absorption studies

In the CO_2 absorption process, CO_2 is removed from the gas phase into a liquid phase by transferring across an interface. Therefore, for the absorption measurement, the CO_2 inlet and outlet concentration are measured by an exhaust gas analyzer. The amount of CO_2 absorbed is calculated by a material balance between the inlet and outlet of the Column. General material

balance is calculated over the testing section of the column by assuming the system is closed and the CO_2 at the inlet is 100%V as follows

$$mass\ of\ CO_2\ inlet - mass\ of\ CO_2 out = mass\ of\ CO_2\ absorbed \tag{3.5}$$

The CO_2 absorption capacity is also defined as how much CO_2 is removed by solution and it's calculated by the mass of CO_2 absorbed per mass of solvent [49].

$$CO_2 \text{ absorption capacity } = \frac{mass\ of\ CO_2\ absorbed}{mass\ of\ solvent} \tag{3.6}$$

The other important parameter that is used to evaluate the absorbent performance is the CO_2 removal efficiency which is the rate of the value of CO_2 removed from the incoming gas to the bubble column. Meanwhile, CO_2 removal efficiency can be calculated by assuming the equal inlet and outlet gas stream, the amount of CO_2 removed does not affect the CO_2 flow rate [1].

$$CO_2 \text{ removal efficiency} = \frac{y_{CO2-in} - y_{CO2-out}}{y_{CO2-in}} x\ 100 \tag{3.7}$$

Where $y_{CO2,inlet}$ and y_{CO2}, out is CO_2 mole fraction at inlet and outlet respectively.

3.8. Hydrodynamic studies

A hydrodynamic study in the bubble column reactor is evaluated by investigating the change in the gas-liquid interfacial area during the carbon dioxide chemical absorption in solutions [31]. One of the most important parameters specifying the bubble columns hydro-dynamics is gas hold up. It was determined based on the method of volume expansion as follows [29, 36, 37, 44].

$$\varepsilon = \frac{\Delta L}{\Delta L + L} \tag{3.8}$$

Where L is the initial liquid level and ΔL is the level expansion after gas dispersion.

The bubble diameter was measured based on the photographic method according to the image analysis of the bubble taken from the column by a digital microscope. The geometrical measurement of the image taken was analyzed by the image tool software package. The diameter

of the single bubbles can be calculated from the area (A) of the bubbles measured by imageJ software.

$$d = \sqrt{4 * A/\pi} \tag{3.9}$$

As many authors recommended the most commonly used bubble size definition is Sauter's mean diameter (d_{32}) that used to get an adequate average diameter.

$$d_{32} = \frac{\sum_{i=1}^{N} n_i d_i^3}{\sum_{i=1}^{N} n_i d_i^2} \tag{3.10}$$

Where d_i and n_i are the diameter of a single bubble and the number of bubbles that have an equivalent diameter (d_i), respectively.

CHAPTER FOUR

RESULT AND DISCUSSION

4.1. Validation of types of reactor Manufactured

Since the bubble column reactor designed for this work is assumed to be a well-mixed flow reactor, the residence time distribution was done to validate this assumption using the sodium chloride step experiment. The experiment was conducted using sodium chloride solution of initial concentration $C_o = 0.2408 mol/m^3$ as a tracer by switching at t= 0 from the ordinary solution to the sodium chloride solution and measuring the outlet concentration with time as shown in Table 4.1.

Table 4.1: The experimental result of the residence time distribution in BCR.

Time(min)	1	2	3	4	5	6	7
Concentration (mol/m^3)	0.02684	0.02764	0.02834	0.02862	0.0289	0.02898	0.02902
Time(min)	8	9	10	11	12	13	14
Concentration (mol/m^3)	0.02906	0.02912	0.0301	0.03672	0.0778	0.1144	0.1458
Time(min)	15	16	17	18	19	20	21
Concentration (mol/m^3)	0.169	0.184	0.1992	0.21	0.02196	0.2234	0.2278
Time(min)	22	23	24	25	26	27	28
Concentration (mol/m^3)	0.232	0.2336	0.236	0.2376	0.2398	0.2404	0.2408
Time(min)	29	30					
Concentration (mol/m^3)	0.2408	0.2408					

Figure 4.1 shows the F-curve of residence time distribution of the bubble column reactor designed in this study. It shows that the reactor has a deviation from the plug flow reactor and shows a dispersion flow reactor.

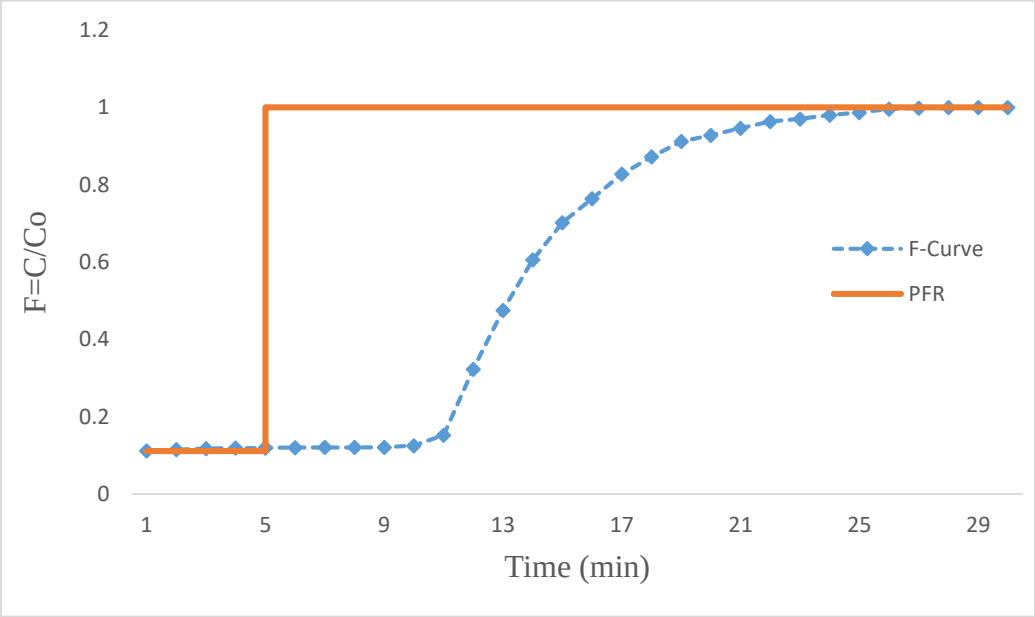

Figure 4.1: The F-curve of the step experiment in the bubble column reactor.

From the experimental data of table (4.1) the dispersion number $\frac{D}{UL}$, is calculated using the meantime of passage ($\dot{t}$), and variance (σ^2). The result obtained is: $\frac{D}{UL} = 0.052$.

Where, $\frac{D}{UL} \rightarrow 0$ negligible dispersion, hence plug flow

$\frac{D}{UL} \rightarrow \infty$ large dispersion hence mixed flow

$\frac{D}{UL} > 0.01$ large deviation from plug flow,

Therefore, the dispersion number obtained indicates a significant deviation from plug flow and proves that the reactor designed is a dispersion flow reactor.

4.2. Micro-bubble size generated

The micro-bubble size generated in this work was measured by using the imageJ software based on the photographic method by taking the image of bubbles from the column using a digital microscope. It was processed from the original image taken by selecting and cleaning as shown in Figure (4.2). And the result obtained from the ImageJ software for the area and diameter of individual bubbles are summarized in Table of Appendix F. Since many authors recommended the most commonly used bubble size definition is Sauter's mean diameter (d_{32}) that used to get an adequate average diameter, the Sauter's mean diameter (d_{32}) calculated from this bubbles was 29.8$\boldsymbol{\mu m}$.

a. 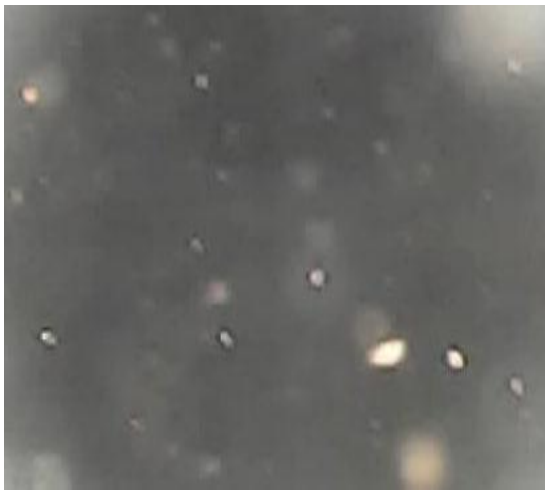 b. 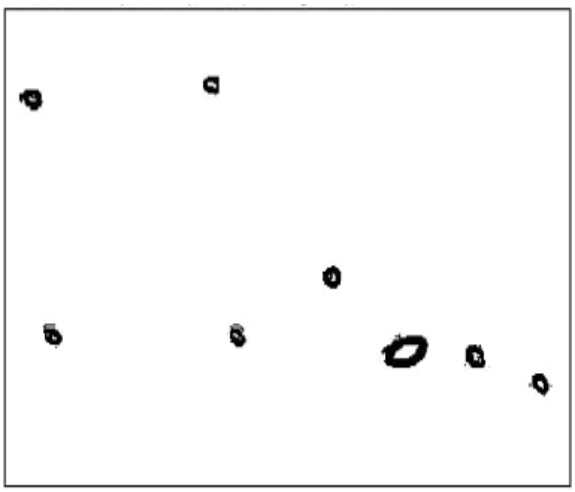

c. 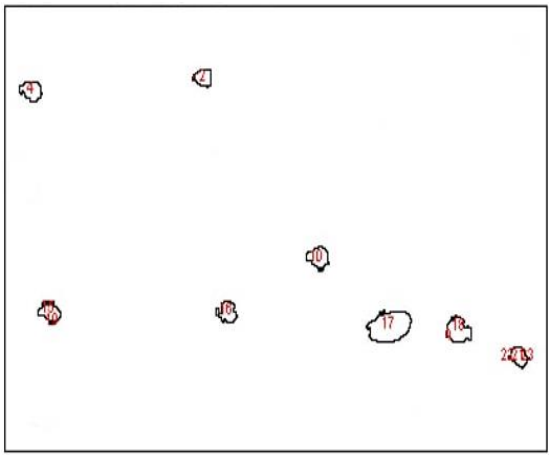

Figure 4.2: Image analysis of micro-bubble size (a). the original image (b) and (c) is modified image.

The image processing technique has also been used to determine the bubble size distribution. Figure 4.3 shows the micro-bubble diameter distribution, which was measured at a height of 0.8m above the nozzle injection.

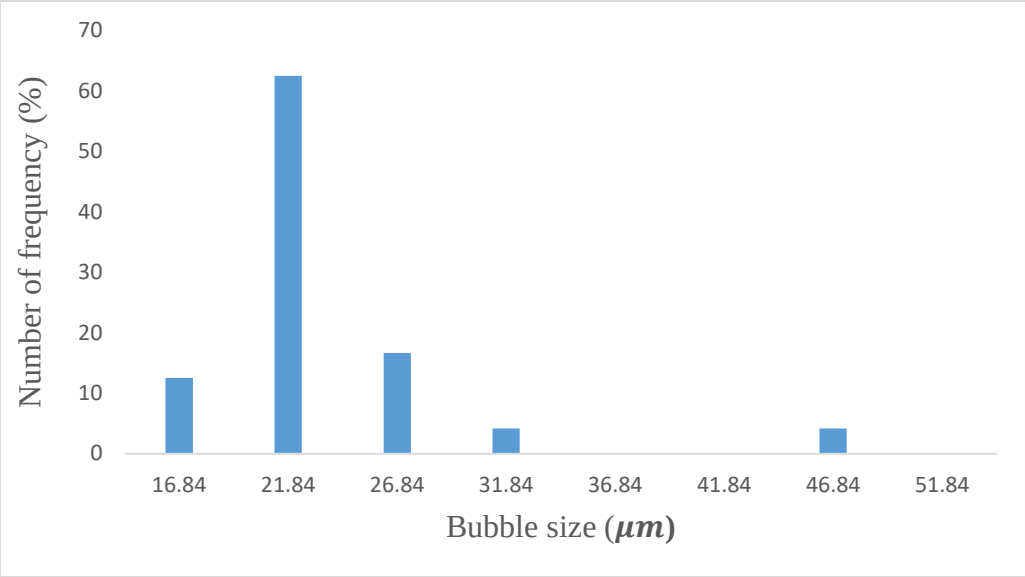

Figure 4.3: Micro-bubble size distribution.

4.3. Effect of solvent concentration on the carbon dioxide outlet

To investigate the effect of solvent concentration on the carbon dioxide outlet, this work was carried out at various solvent concentrations. Figure (4.4) shows the effect of ammonia solution concentration on the carbon dioxide outlet concentration at the same carbon dioxide flow rates (1.5L/min) and operating time. The result shows that the carbon dioxide concentration at the outlet increased with the operation time for all the ammonia concentration and the carbon dioxide concentration at the outlet decreased when the ammonia concentration was increased from 1% to 7% (v/v). The reason is that the increase of the solvent concentration gives a higher amount of the active solvent available to diffuse toward the gas-liquid interface and react with carbon dioxide.

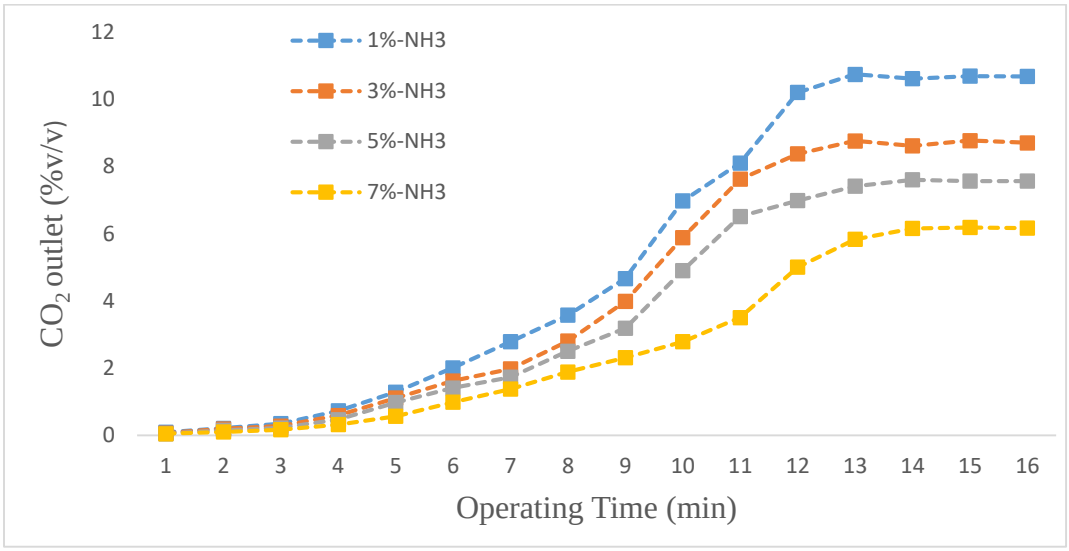

Figure 4.4: The effect of ammonia concentration on the carbon dioxide outlet at carbon dioxide flow rates 1.5L/min.

Figure (4.5) shows the effect of sodium hydroxide solution concentration on the carbon dioxide outlet concentration at the same carbon dioxide flow rates (1.5L/min) and operating time. The result shows that the carbon dioxide concentration at the outlet increased with the operation time for all the sodium hydroxide concentrations and the carbon dioxide concentration at the outlet decreased when the sodium hydroxide concentration was varied from 1% to 7% (v/v).

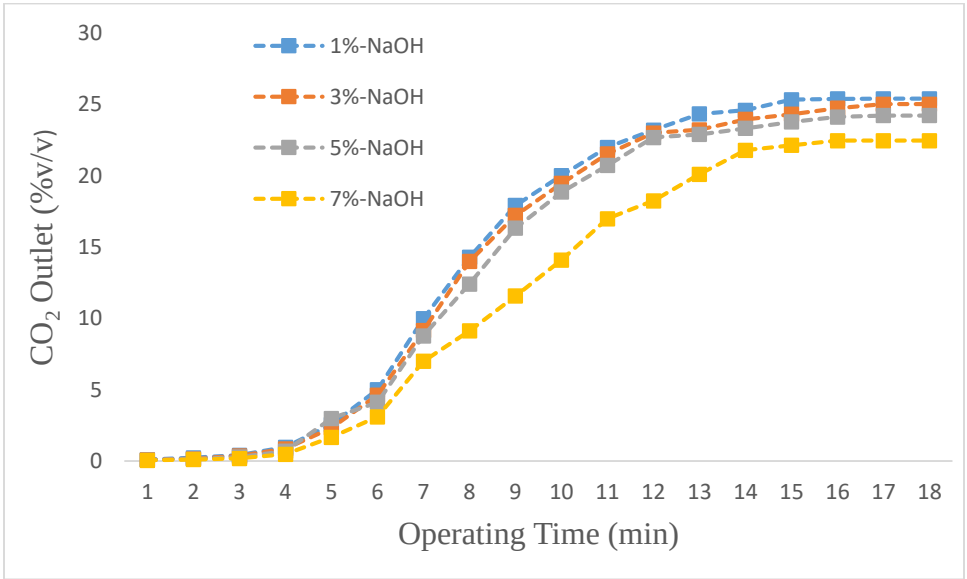

Figure 4.5: The effect of sodium hydroxide concentration on the carbon dioxide outlet at carbon dioxide flow rates 1.5L/min.

Figure (4.6) shows the effect of mono-ethanolamine solution concentration on the carbon dioxide outlet concentration at the same carbon dioxide flow rates (1.5L/min) and operating time. Similar to that of the ammonia and sodium hydroxide the carbon dioxide outlet concentration was increased with the operation time for all the mono-ethanolamine concentrations.

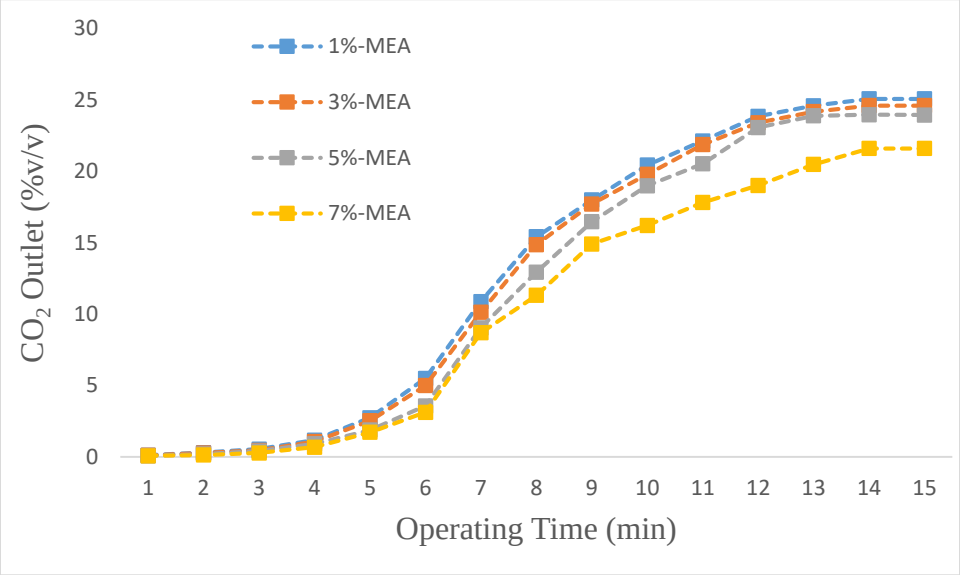

Figure 4.6: The effect of mono-ethanolamine concentration on the carbon dioxide outlet at carbon dioxide flow rates 1.5L/min.

4.4. Effect of the operating time on the carbon dioxide outlet mole fraction

Figure (4.7) shows the change of CO_2 outlet mole fraction as the function of operating time using CO_2 micro-bubbles for NH_3, NaOH, and MEA as an absorbent in a bubble column reactor. The column was operated at a CO_2 inlet concentration of 100 (%V/V), a CO_2 flow rate of 1.5L/min, and solvent concentration of 3% (V/V) for the NH_3, NaOH, and MEA solvent. As shown on the graph the amount of CO_2 on the outlet increased with increased operating time for all the solvents. The time with maximum absorption for ammonia solvent is approximately the first 120s. This is similar to the time reported by Zhao et.al. 2013 [2] work performed with different reaction parameters and time range of 60-360s. At that time the CO_2 concentration at the outlet was 0.07%

(V/V) which corresponds to a high removal efficiency of 99.9%, and the high removal efficiency was maintained for 5min.

Similarly, the maximum absorption during the first 1min resulted in a CO_2 outlet concentration of 0.09% (V/V) and 0.08 % (V/V) respectively for sodium hydroxide and the mono-ethanolamine solution. For both solvents, the corresponding maximum removal efficiency of 99.9% was equal for both solvents. This indicates both solvents have a fast reaction rate with CO_2.

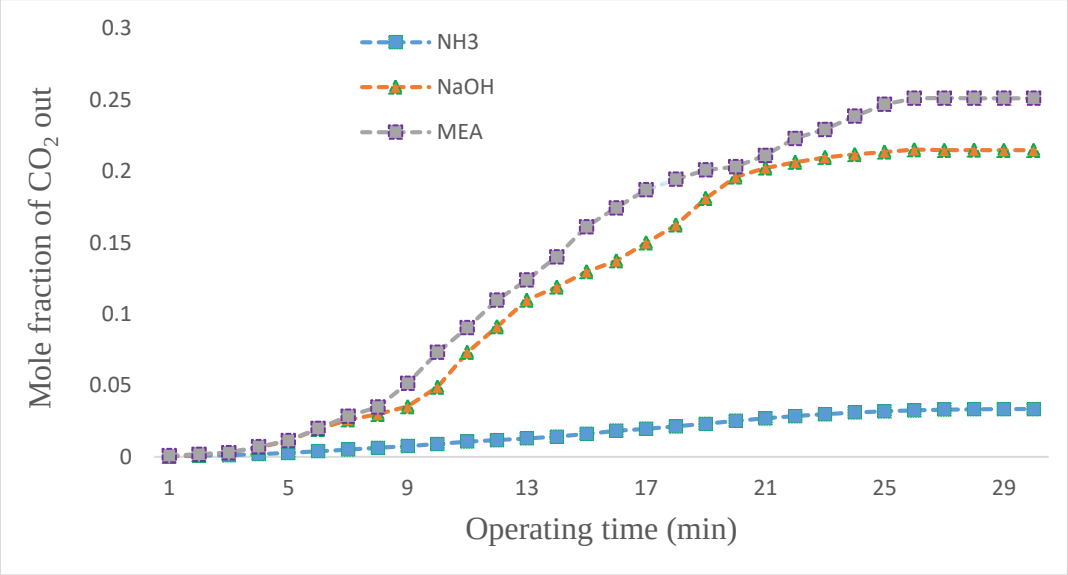

Figure 4.7: Change of CO_2 mole fraction with operating time using CO_2 micro-bubbles (at CO_2 inlet concentration of 100 (%V/V), a CO_2 flow rate of 1.5L/min, and solvent concentration of 3% (V/V)).

Figure (4.8) shows the change of CO_2 outlet mole fraction as the function of operating time using CO_2 conventional bubbles for NH_3, NaOH, and MEA as an absorbent in a bubble column reactor with the same operating condition to the CO_2 micro-bubbles. Similarly, the mole fraction of CO_2 at the outlet increased with increasing of the operating time in the case of CO_2 conventional bubbles. However, it reached a maximum value within a shorter time for CO_2 conventional bubble assisted system. The reason is that the absorption time depends on the bubble size and it shows that, when the bubble size increase the contacting time of the CO_2 and the solvent is low decreasing the efficiency of the mass transfer from the gas phase to the liquid phase because of the fast movement of the big bubbles.

In general, the time required to reach maximum CO_2 absorption in BCR for both micro-bubbles and conventional bubbles depends on the tested operating parameters and bubble size.

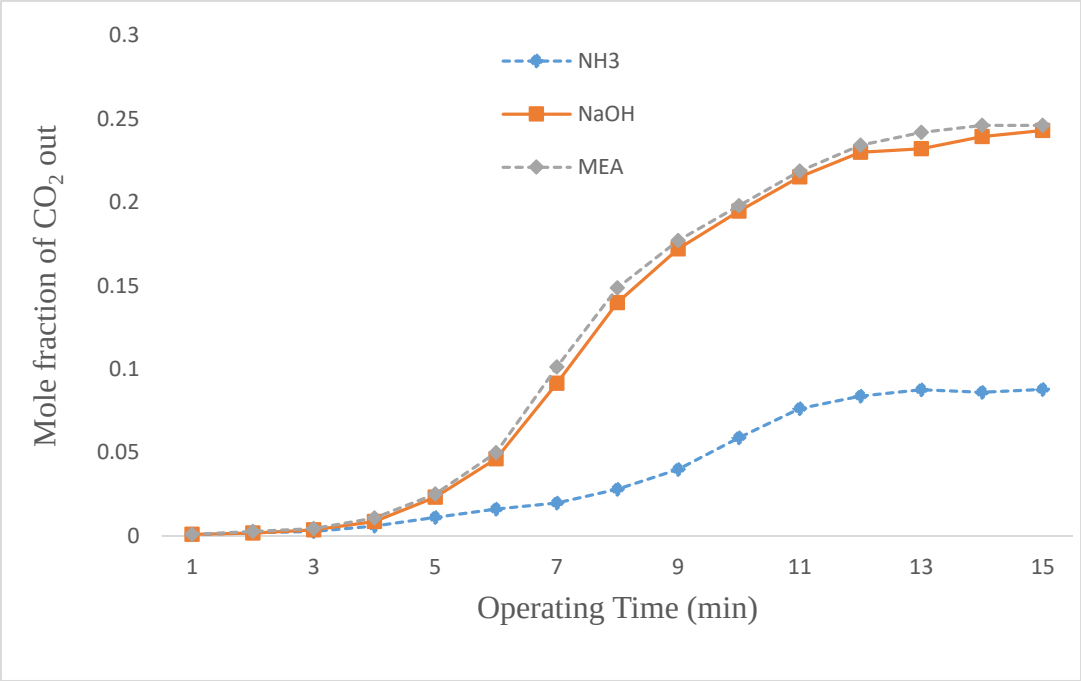

Figure 4.8: Change of CO_2 mole fraction with operating time using CO_2 conventional bubbles (at CO_2 inlet concentration of 100 (%V/V), a CO_2 flow rate of 1.5L/min, and solvent concentration of 3% (V/V)).

4.5. Effect of the solvent concentration on the carbon dioxide removal efficiency

A comparison on the performance of the solvents on the CO_2 removal efficiency profile for different concentrations of NH_3, NaOH, and MEA using CO_2 micro-bubbles is shown in Figure (4.9). In this case, the operating condition was at a CO_2 flow rate of 1.5L/min, and the concentration of CO_2 at the inlet was 100% (v/v). The solvent concentration for both NH_3, NaOH, and MEA is 1, 3, 5, and 7%.

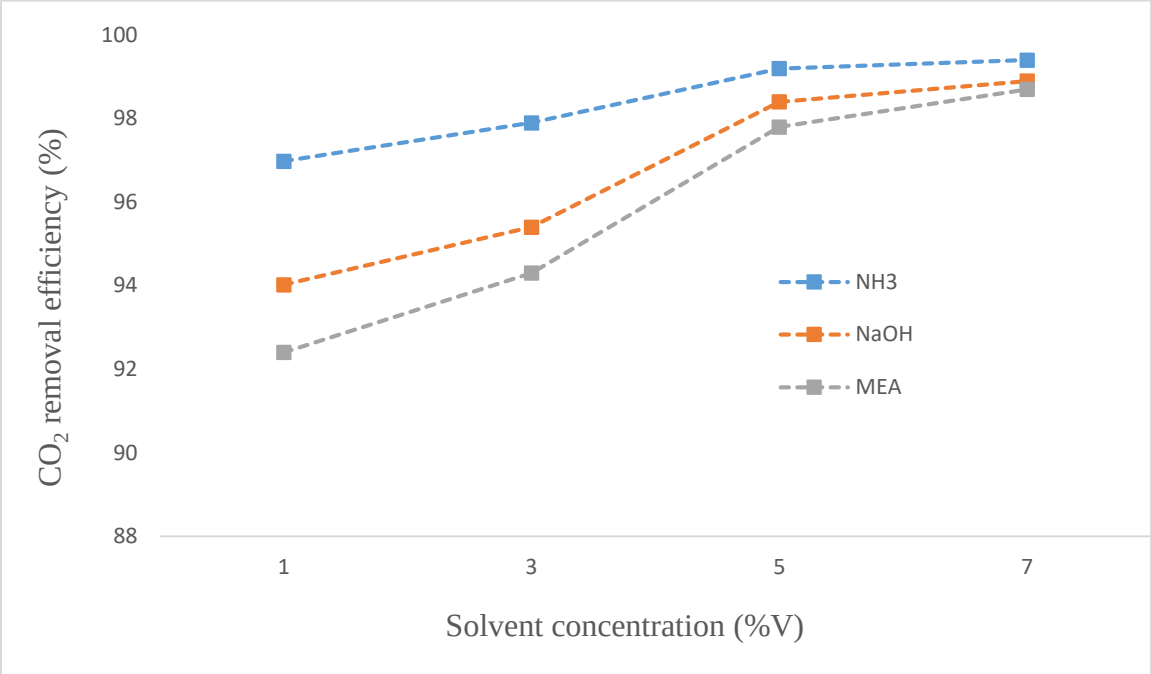

Figure 4.9: The effect of solvent concentration on CO_2 removal efficiency using CO_2 micro-bubbles (at CO_2 flow rate of 1.5L/min).

It is seen that the solvent concentration plays an important role in the CO_2 removal efficiency. The maximum CO_2 removal efficiencies using NH_3 solvent increase from 96.9 to 99.4% as ammonia concentration varies from 1% to 7% (V/V). The maximum CO_2 removal efficiencies for NaOH solvent increase from 94.02 to 98.9% as sodium hydroxide concentration varies from 1% to 7% (V/V). While the maximum CO_2 removal efficiencies for MEA solvent increase from 92.4 to 98.4% as MEA concentration varies from 1% to 7% (V/V). This is because increasing solvent concentration gives a higher amount of the active solvent available to diffuse towards the gas-liquid interface and react with carbon dioxide. In other way when the solvent concentration is high, the absorption is very fast because the conversion is high. By comparison between the selected chemicals, NH_3 exhibited the maximum absorption efficiency compared to all the three chemicals. NaOH and MEA take the next consecutive ranks respectively.

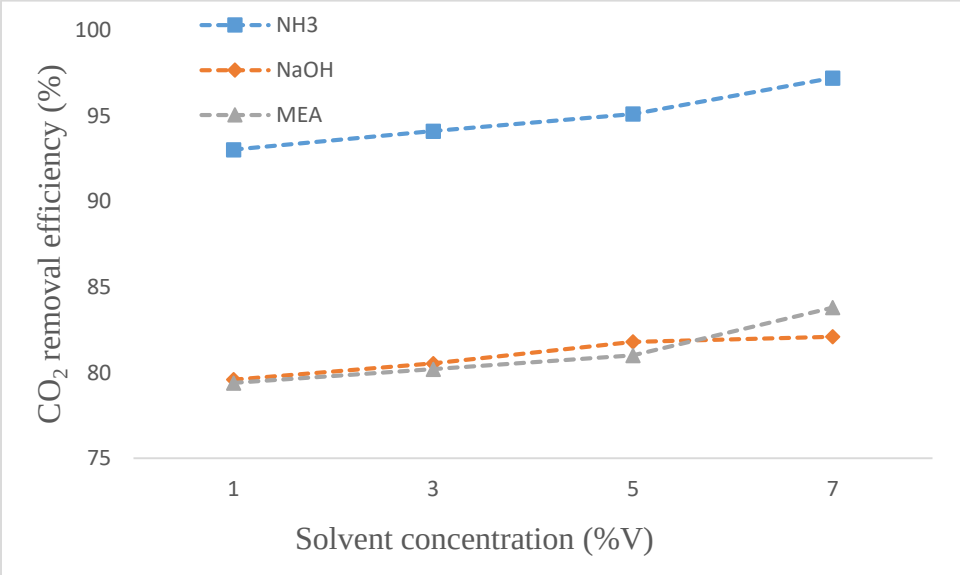

Figure 4.10: The effect of solvent concentration on CO_2 removal efficiency using CO_2 conventional bubbles (at CO_2 flow rate of 1.5L/min).

Figure (4.10) shows the performance of the solvents on the CO_2 removal efficiency profile for different concentrations of NH_3, NaOH, and MEA using CO_2 conventional bubbles. Similar to the CO_2 micro-bubbles the CO_2 removal efficiency of all solvent using CO_2 conventional bubbles increases with increasing solvent concentration. The CO_2 removal efficiencies using NH_3 solvent increase from 93.02 to 97.2% as ammonia concentration varies from 1% to 7% (V/V). The CO_2 removal efficiencies for NaOH solvent increase from 79.6 to 82.1% as sodium hydroxide concentration varies from 1% to 7% (V/V). While CO_2 removal efficiencies for MEA solvent increase from 79.4 to 83.79 as MEA concentration varies from 1% to 7% (V/V). Comparing the removal efficiencies of the conventional bubble assisted system (Figure 4.10) and the micro bubble assisted system (Figure 4.9), the CO_2 removal efficiencies for both CO_2 micro-bubbles and CO_2 conventional bubbles was increased with increasing solvent concentration. However, the removal efficiencies of the micro-bubble assisted are more efficient than the conventional bubble assisted system specially for the relatively slow reactive solvents NaOH and MEA. This is because smaller bubbles have a higher gas-liquid specific surface area, slow rising velocity in the solution due to the low buoyancy force and high dissolution rate [40], which contribute for the increase in mass transfer by delivering enough reaction surface and time of contact between phases.

4.6. Effect of carbon dioxide flow rate on carbon dioxide removal efficiency

Figure (4.11) shows the result of CO_2 removal efficiencies in NH_3, NaOH, and MEA using the CO_2 micro-bubbles with a range of CO_2 flow rates. The effect of CO_2 flow rate was evaluated in this work by varying it from 1 to 2.5L/min at 100% (v/v) inlet concentration of CO_2, and 3% (V/V) solvent concentration for NH_3, NaOH, and MEA.

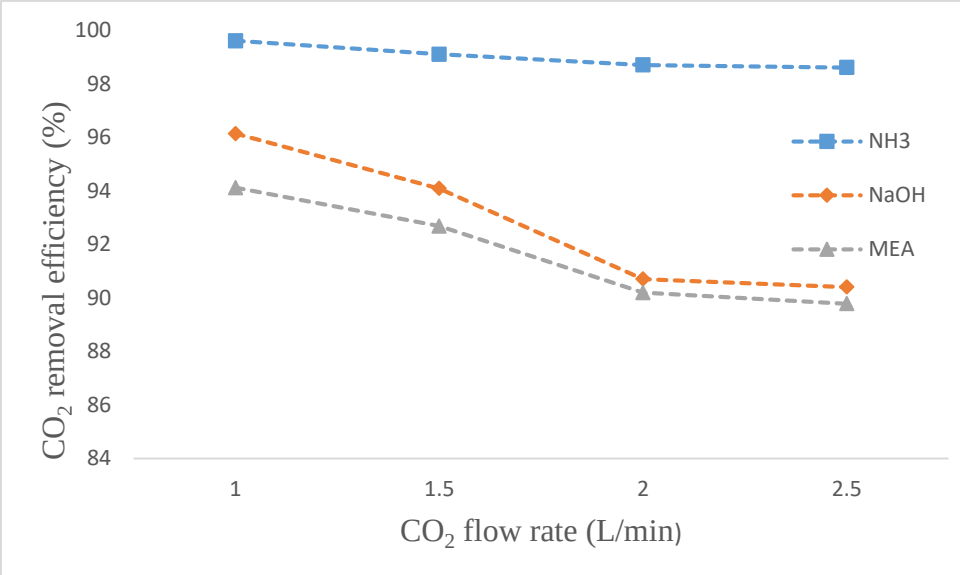

Figure 4.11: The effect of the CO_2 flow rate on the CO_2 removal efficiency using the CO_2 micro-bubbles (at 3% (V/V) solvent concentration for NH_3, NaOH, and MEA).

The experimental result showed that the CO_2 removal efficiency decreased as the CO_2 flow rate was increased from 1 to 2.5L/min for all of the solvents. When using ammonia solvent, the CO_2 removal efficiencies decreased from 99.6 to 98.6% as the CO_2 flow rate was increased from 1 to 2.5L/min. Similarly, using sodium hydroxide solvent, the CO_2 removal efficiency decreased from 96.13 to 90.4% as the CO_2 flow rate was increased from 1 to 2.5L/min. When using MEA solvent, the CO_2 removal efficiency decreased from 94.11 to 89.78% as the CO_2 flow rate was increased from 1 to 2.5L/min.

In similar manner, Figure (4.12) shows the result of CO_2 removal efficiencies in NH_3, NaOH, and MEA using the CO_2 conventional bubbles with a range of CO_2 flow rates. The CO_2 removal efficiency decreased as the CO_2 flow rate was increased from 1 to 2.5L/min for all of the solvents

in case of conventional bubbles. Using ammonia solvent as a sequesterant, CO_2 removal efficiency decreased from 94.59 to 93.69% while it was decrease from 80.88 to79.2% and 81.16 to 78.88% for NaOH and MEA for an increase of the CO_2 flow rate from 1 to 2.5L/min.

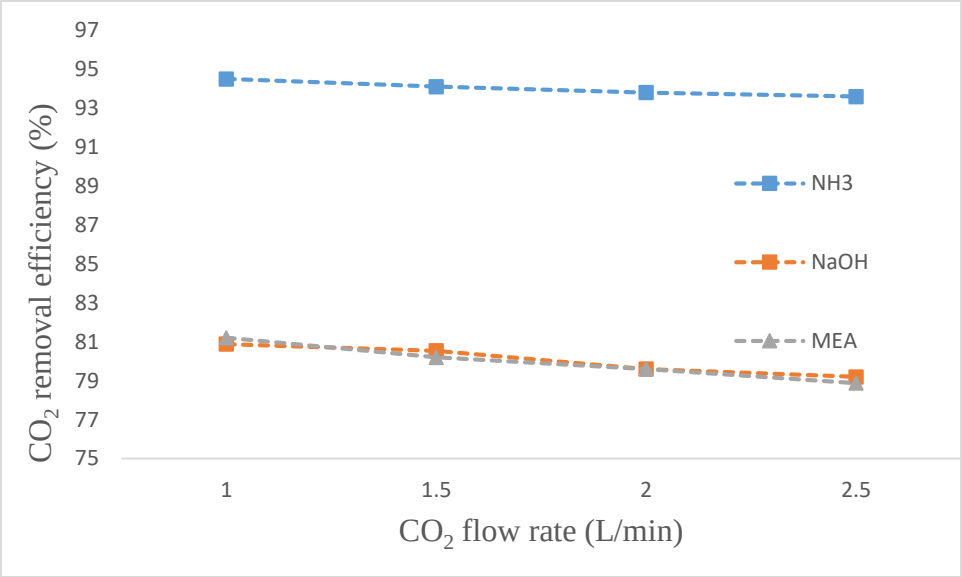

Figure 4.12: The effect of CO_2 flow rate on CO_2 removal efficiency using the CO_2 Conventional bubbles (3% (V/V) solvent concentration for NH_3, NaOH, and MEA).

The main reason for decreasing of CO_2 removal efficiency as the CO_2 flow rate was increased is that the reaction time between the solvent and CO_2 becomes insufficient, since the increasing of the CO_2 flow rate increase the superficial velocity of carbon dioxide bubbles through the bulk solution and decrease the staying time in the bulk. At the same time, increasing the CO_2 flow rate leads to decreases in the carbon dioxide to solvent mole ratio.

4.7. Effect of the superficial velocity on the carbon dioxide holdup

CO_2 holdup is the amount of volume fraction of gas-phase occupied by the CO_2 bubbles. Since the gas holdup in the bubble column is mainly dependent on the gas superficial velocity, this study was conducted to assess the influence of CO_2 superficial velocity on the CO_2 holdup by using CO_2 micro-bubble and conventional bubbles. Figure (4.13) shows the result of the superficial velocity effect on CO_2 holdup for 3% (V/V) solvent concentration of NH_3, NaOH, and MEA in bubble column using CO_2 micro-bubbles. The CO_2 holdup for ammonia solvent increased from 0.0049 to

0.0099 as the superficial velocity was increased from 1.67 mm/s to 4.17 mm/s, while it was from 0.0043 to 0.0092 and 0.0031 to 0.008 for NaOH and MEA respectively, as the superficial velocity was increased from 1.67 mm/s to 4.17 mm/s.

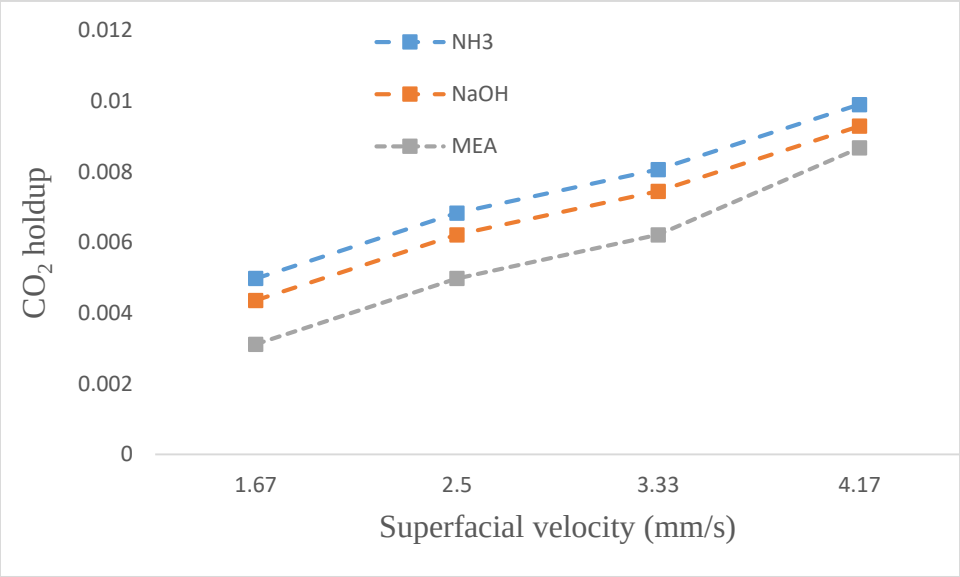

Figure 4.13: The effect of superficial velocity on CO_2 holdup using CO_2 micro-bubble size.

Figure (4.14) also shows the effect of the superficial velocity on CO_2 holdup for conventional bubbles size with the same solvent concentration of NH_3, NaOH, and MEA in bubble column to that of CO_2 micro-bubble size.

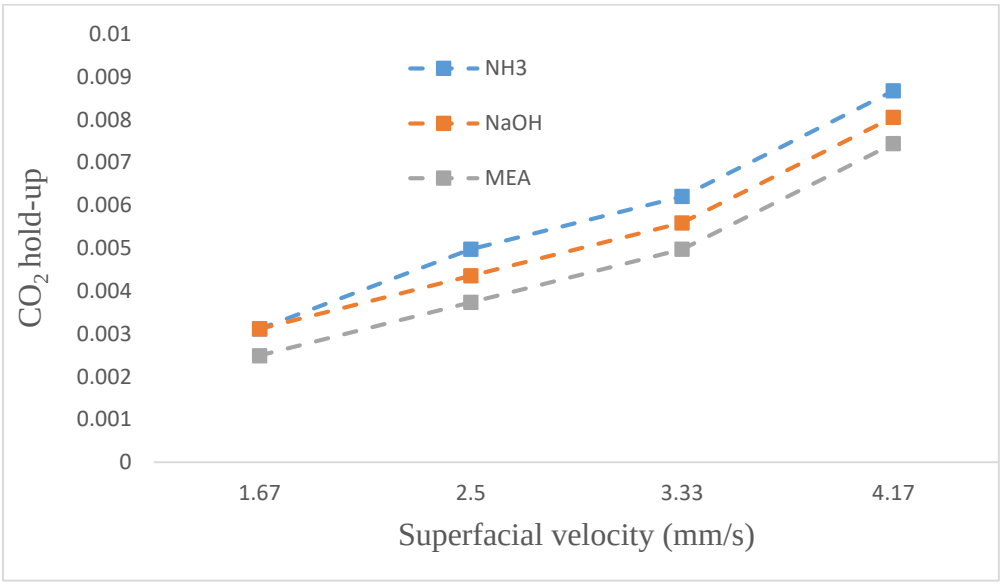

Figure 4.14: The effect of superficial velocity on CO_2 holdup using CO_2 conventional bubble size.

The result shows that for the CO_2 conventional bubbles, the CO_2 holdup for ammonia solvent is increased from 0.0031 to 0.009 as the superficial velocity was increased from 1.67 mm/s to 4.17 mm/s, while it was from 0.0031 to 0.0082 and 0.0024 to 0.0074 for NaOH and MEA respectively, as the superficial velocity was increased from 1.67 mm/s to 4.17 mm/s. It is seen that the superficial velocity plays an important role in the CO_2 holdup. The CO_2 holdup was increased with increasing superficial velocity. This is because of the higher volume of CO_2 in the bubble column as the CO_2 flow rate or superficial velocity is increased, while the volume of the solvent is constant, which leads to an increase of CO_2 to solvent ratio which reduces the removal efficiency.

General, the experimental result shows that the CO_2 holdup for the CO_2 micro-bubble assisted system was higher than that of the CO_2 conventional bubble assisted system. The reason is that the gas holdup is also depending on the diameter of the gas bubbles which is the CO_2 holdup is high when the number of bubbles is high and their diameter is small.

Table 4.2: The Comparison of this work to previous works of literature

Equipment used	Solvent	Operating Condition	Result	Author
Bubble column reactor (H=159.2 mm and D=40mm)	Ammonia	Bubble size=1.5mm NH_3 (14%w/w) Gas flow rate =1.5L/min) Time=20min	CO_2 capture efficiency = 98.89%	[2]
Semi-continuous flow Reactor (H=120mm, D=60mm and V=20ml)	Ammonia and MEA	CO_2 concentration=99.9%, Gas flow rate (2-10L/min, and solvent (7-35%) (w/w)	CO_2 capture efficiency (48-99% for NH_3 and 42-92 for MEA)	[50]
Bubble column reactor H/D ratio=0.87, 1.51, 2.32, 3, 4.28, 5.76	Ammonia	CO_2 Concentration (10-20%), Gas flow rate (6(m/min/m2), NH3 (4-8) (kmol/m3)	CO_2 capture efficiency increase with H/D increase	[1]
Fine spray Column (H=1300mm, D=120mm)	Ammonia and Sodium hydroxide	Gas flow rate (7.6-24.7L/min), solvent concentration (2-10%w/w), CO_2 inlet (15%v/v)	CO_2 capture efficiency increase with solvent and gas flow rate ($NaOH<NH_3$).	[51]
Bubble column Reactor (H=1000mm, L=100mm,W=100mm)	Ammonia, sodium hydroxide and MEA	CO_2 Concentration (100%), solvent concentration (1-7%v/v), Gas flow rate (1-2.5L/min), micro-bubble and conventional bubble.	CO_2 capture efficiency increase with bubble size reduction and decrease with gas flow rate.	This work

CHAPTER FIVE

CONCLUSION AND RECOMMENDATION

5.1. Conclusion

In this work the rectangular bubble column reactor from acrylic glass with a square cross-sectional area of (WxL) of 0.1x0.1 m^2 and a height of 1m were designed and manufactured. From the experimental result, the assumption for the design of the reactor was proved by the RTD result analysis and found out that $\frac{D}{UL} = 0.052$ which shows that the flow pattern follows dispersion flow/mixed flow reactor. The venturi supported splitter type micro-bubble generator was also designed and manufactured to generate the CO_2 micro-bubbles. The result obtained from the ImageJ software shows Sauter's mean diameter (d_{32}) of micro-bubble generated was 29.8μm.

The absorption of carbon dioxide using Ammonia, Sodium hydroxide, and Mono-ethanolamine solution was investigated experimentally in a bubble column reactor. The solvents concentration and CO_2 flow rate studied were 1 - 7% (v/v), and 1 - 2.5L/min respectively. The performance of those solvents is compared in terms of the CO_2 removal efficiency. The experimental data showed that the CO_2 removal efficiency of ammonia solution is better than that of sodium hydroxide and mono-ethanolamine solution under the operating condition of this study. What's more the CO_2 removal efficiency of all the solvent increase with increasing the solvent concentration from 1 to 7% (V/V) and decrease with increasing the CO_2 flow rate from 1 to 2.5L/min.

This work is also tried to investigate the effect of the CO_2 superficial velocity on the CO_2 holdup. The result obtained showed that the CO_2 hold up for all the solvents increase with increasing the CO_2 superficial velocity. The reason is that the higher volume of CO_2 in the bubble column as the CO_2 flow rate/superficial velocity is increased, while the volume of the solvent is constant, leads to increase CO_2 gas to solvent ratio.

Additionally, the effect of the bubble size on the CO_2 removal efficiency using systems assisted by CO_2 micro-bubble generator and CO_2 conventional bubbles generator. It was found out that CO_2 removal efficiency of all the solvents using micro-bubbles was better than that of the conventional bubbles because the smaller bubbles have a high gas-liquid specific surface area,

slow rising velocity in the solution due to the low buoyancy force, and high dissolution rate so that they could have a high removal efficiency.

5.2. Recommendation

Based on the outcomes of this work, the following recommendations are suggested for future research which is related to the carbon dioxide absorption in a bubble column reactor.

- From the reactor design point of view, the reactor shall be designed or modified with the temperature control system for detailed study of the reaction kinetics and mass transfer coefficient of Carbon dioxide with the solvents.
- Further research on the effect of different hydrodynamic bubble column reactor types for the comparison of the carbon dioxide absorption.
- Since this work used different solvents for carbon dioxide absorption without the solvent regeneration, further study may focus on the best ways of regenerating the solvents during carbon dioxide absorption.

REFERENCE

[1] F. Chu, L. Yang, X. Du, and Y. Yang, "Mass transfer and energy consumption for CO_2 absorption by ammonia solution in bubble column," *Appl. Energy*, vol. 190, pp. 1068–1080, 2017, doi: 10.1016/j.apenergy.2017.01.027.

[2] B. Zhao, Y. Su, and Y. Peng, "Effect of reactor geometry on aqueous ammonia-based carbon dioxide capture in bubble column reactors," *Int. J. Greenh. Gas Control*, vol. 17, no. x, pp. 481–487, 2013, doi: 10.1016/j.ijggc.2013.06.009.

[3] C. H. Hsu, H. Chu, and C. M. Cho, "Absorption and reaction kinetics of amines and ammonia solutions with carbon dioxide in flue gas," *J. Air Waste Manag. Assoc.*, vol. 53, no. 2, pp. 246–252, 2003, doi: 10.1080/10473289.2003.10466139.

[4] T. H. Oh, "Carbon capture and storage potential in coal-fired plant in Malaysia - A review," *Renew. Sustain. Energy Rev.*, vol. 14, no. 9, p. 2697, 2010, doi: 10.1016/j.rser.2010.06.003.

[5] D. Y. C. Leung, G. Caramanna, and M. M. Maroto-Valer, "An overview of current status of carbon dioxide capture and storage technologies," *Renew. Sustain. Energy Rev.*, vol. 39, pp. 426–443, 2014, doi: 10.1016/j.rser.2014.07.093.

[6] Intergovernmental Panel on Climate Change (IPCC), *Climate change 2007: Synthesis report*. 2008.

[7] J. Liu, S. Wang, B. Zhao, H. Tong, and C. Chen, "Absorption of carbon dioxide in aqueous ammonia," *Energy Procedia*, vol. 1, no. 1, pp. 933–940, 2009, doi: 10.1016/j.egypro.2009.01.124.

[8] B. Zhao, W. Tao, M. Zhong, Y. Su, and G. Cui, "Process, performance and modeling of CO_2 capture by chemical absorption using high gravity: A review," *Renew. Sustain. Energy Rev.*, vol. 65, pp. 44–56, 2016, doi: 10.1016/j.rser.2016.06.059.

[9] P. Mores, N. Scenna, and S. Mussati, "CO_2 capture using monoethanolamine (MEA) aqueous solution: Modeling and optimization of the solvent regeneration and CO_2 desorption process," *Energy*, vol. 45, no. 1, pp. 1042–1058, 2012, doi: 10.1016/j.energy.2012.06.038.

[10] J. Lee, T. Kolawole, and P. Attidekou, "Carbon Capture from a Simulated Flue Gas Using a Rotating Packed Bed Adsorber and Mono Ethanol Amine (MEA)," *Energy Procedia*, vol. 114, no. November 2016, pp. 1834–1840, 2017, doi: 10.1016/j.egypro.2017.03.1312.

[11] H. Pashaei, M. N. Zarandi, and A. Ghaemi, "Experimental study and modeling of CO_2 absorption into diethanolamine solutions using stirrer bubble column," *Chem. Eng. Res. Des.*, vol. 121, pp. 32–43, 2017, doi: 10.1016/j.cherd.2017.03.001.

[12] A. Aroonwilas, P. Tontiwachwuthikul, and A. Chakma, "Effects of operating and design parameters on CO_2 absorption in columns with structured packings," *Sep. Purif. Technol.*,

vol. 24, no. 3, pp. 403–411, 2001, doi: 10.1016/S1383-5866(01)00140-X.

[13] W. Shi *et al.*, "Modelling of mass transfer for gas-liquid two-phase flow in bubble column reactor with a bubble breakage model considering bubble-induced turbulence," *Chem. Eng. J.*, vol. 371, no. April, pp. 470–485, 2019, doi: 10.1016/j.cej.2019.04.047.

[14] M. Zhang and Y. Guo, "Process simulations of NH_3 abatement system for large-scale CO_2 capture using aqueous ammonia solution," *Int. J. Greenh. Gas Control*, vol. 18, pp. 114–127, 2013, doi: 10.1016/j.ijggc.2013.07.005.

[15] Y. Wang, L. Zhao, A. Otto, M. Robinius, and D. Stolten, "A Review of Post-combustion CO_2 Capture Technologies from Coal-fired Power Plants," *Energy Procedia*, vol. 114, no. November 2016, pp. 650–665, 2017, doi: 10.1016/j.egypro.2017.03.1209.

[16] P. Luis, "Use of monoethanolamine (MEA) for CO_2 capture in a global scenario: Consequences and alternatives," *Desalination*, vol. 380, pp. 93–99, 2016, doi: 10.1016/j.desal.2015.08.004.

[17] R. Rivera-Tinoco and C. Bouallou, "Comparison of absorption rates and absorption capacity of ammonia solvents with MEA and MDEA aqueous blends for CO_2 capture," *J. Clean. Prod.*, vol. 18, no. 9, pp. 875–880, 2010, doi: 10.1016/j.jclepro.2009.12.006.

[18] M. Yoo, S. Han, and J. Wee, "Carbon dioxide capture capacity of sodium hydroxide aqueous solution," *J. Environ. Manage.*, vol. 114, pp. 512–519, 2013, doi: 10.1016/j.jenvman.2012.10.061.

[19] N. Kantarci, F. Borak, and K. O. Ulgen, "Bubble column reactors," *Process Biochem.*, vol. 40, no. 7, pp. 2263–2283, 2005, doi: 10.1016/j.procbio.2004.10.004.

[20] P. Sastaravet, C. Chuenchaem, N. Thaphet, N. Chawaloesphonsiya, and P. Painmanakul, "Comparative study of mass transfer and bubble hydrodynamic parameters in bubble column reactor: Physical configurations and operating conditions," *Environ. Eng. Res.*, vol. 19, no. 4, pp. 345–354, 2014, doi: 10.4491/eer.2014.S1.013.

[21] A. K. Verma and C. Nayak, "Acoustic measurement in a rectangular bubble column to determine bubble size and interfacial area for aqueous solutions of ethylene glycol," *Int. J. Recent Technol. Eng.*, vol. 8, no. 2, pp. 994–998, 2019, doi: 10.35940/ijrte.B1794.078219.

[22] M. A. S. Mohd Yunos, S. A. Hussain, H. Mohamed Yusoff, and S. Sipaun, "Design and fabrication of quadrilateral bubble column test rig for multiphase flow investigations," no. January, 2017, doi: 10.21276/sjet.2017.5.2.1.

[23] M. Garcia, H. K. Knuutila, and S. Gu, "ASPEN PLUS simulation model for CO_2 removal with MEA: Validation of desorption model with experimental data," *J. Environ. Chem. Eng.*, vol. 5, no. 5, pp. 4693–4701, 2017, doi: 10.1016/j.jece.2017.08.024.

[24] H. Yang *et al.*, "Progress in carbon dioxide separation and capture: A review," *J. Environ. Sci.*, vol. 20, no. 1, pp. 14–27, 2008, doi: 10.1016/S1001-0742(08)60002-9.

[25] P. H. M. Feron and C. A. Hendriks, "CO_2 capture process principles and costs," *Oil Gas Sci. Technol.*, vol. 60, no. 3, pp. 451–459, 2005, doi: 10.2516/ogst:2005027.

[26] M. Abu-Khader, "Recent progress in CO_2 capture/sequestration: A review," *Energy Sources, Part A Recover. Util. Environ. Eff.*, vol. 28, no. 14, pp. 1261–1279, 2006, doi: 10.1080/009083190933825.

[27] C. H. Yu, C. H. Huang, and C. S. Tan, "A review of CO_2 capture by absorption and adsorption," *Aerosol Air Qual. Res.*, vol. 12, no. 5, pp. 745–769, 2012, doi: 10.4209/aaqr.2012.05.0132.

[28] G. Hu, K. H. Smith, Y. Wu, K. A. Mumford, S. E. Kentish, and G. W. Stevens, "Carbon dioxide capture by solvent absorption using amino acids: A review," *Chinese J. Chem. Eng.*, vol. 26, no. 11, pp. 2229–2237, 2018, doi: 10.1016/j.cjche.2018.08.003.

[29] P. S. Nair and P. P. Selvi, "Absorption of Carbon dioxide in Packed Column," *Int. J. Sci. Res. Publ.*, vol. 4, no. 1, pp. 2250–3153, 2014, [Online]. Available: www.ijsrp.org.

[30] A. Aboudheir, P. Tontiwachwuthikul, A. Chakma, and R. Idem, "Kinetics of the reactive absorption of carbon dioxide in high CO_2-loaded, concentrated aqueous monoethanolamine solutions," *Chem. Eng. Sci.*, vol. 58, no. 23–24, pp. 5195–5210, 2003, doi: 10.1016/j.ces.2003.08.014.

[31] H. Pashaei, A. Ghaemi, and M. Nasiri, "Experimental investigation of CO_2 removal using Piperazine solution in a stirrer bubble column," *Int. J. Greenh. Gas Control*, vol. 63, no. February, pp. 226–240, 2017, doi: 10.1016/j.ijggc.2017.05.004.

[32] K. J. H. George, "Investigations in Hydrodynamics and Mixing Pattern in the Bubble Column Equipped with Internals," no. Electronic Thesis and Dissertation Repository. Paper 3167, 2015.

[33] J. J. Romanainen, "I-," vol. 36, 1997.

[34] C. L. Hyndman, F. Larachi, and C. Guy, "Understanding gas-phase hydrodynamics in bubble columns: A convective model based on kinetic theory," *Chem. Eng. Sci.*, vol. 52, no. 1, pp. 63–77, 1997, doi: 10.1016/S0009-2509(96)00387-9.

[35] A. Shaikh and M. H. Al-Dahhan, "A review on flow regime transition in bubble columns," *Int. J. Chem. React. Eng.*, vol. 5, 2007, doi: 10.2202/1542-6580.1368.

[36] C. Leonard, J. H. Ferrasse, O. Boutin, S. Lefevre, and A. Viand, *Bubble column reactors for high pressures and high temperatures operation*, vol. 100. Institution of Chemical Engineers, 2015.

[37] H. Chaumat, A. M. Billet-Duquenne, F. Augier, C. Mathieu, and H. Delmas, "Mass transfer in bubble column for industrial conditions - Effects of organic medium, gas and liquid flow rates and column design," *Chem. Eng. Sci.*, vol. 60, no. 22, pp. 5930–5936, 2005, doi: 10.1016/j.ces.2005.04.026.

[38] R. Demol, D. Vidal, S. Shu, F. Bertrand, and J. Chaouki, “Mass transfer in the homogeneous flow regime of a bubble column,” *Chem. Eng. Process. - Process Intensif.*, vol. 144, no. August, p. 107647, 2019, doi: 10.1016/j.cep.2019.107647.

[39] M. Heydarifard, H. Pashaei, A. Ghaemi, and M. Nasiri, “Reactive absorption of CO_2 into Piperazine aqueous solution in a stirrer bubble column: Modeling and experimental,” *Int. J. Greenh. Gas Control*, vol. 79, no. April, pp. 91–116, 2018, doi: 10.1016/j.ijggc.2018.09.017.

[40] T. Temesgen, T. T. Bui, M. Han, T. il Kim, and H. Park, “Micro and nanobubble technologies as a new horizon for water-treatment techniques: A review,” *Adv. Colloid Interface Sci.*, vol. 246, no. June, pp. 40–51, 2017, doi: 10.1016/j.cis.2017.06.011.

[41] J. Huang *et al.*, “A review on bubble generation and transportation in Venturi-type bubble generators,” vol. 2, no. 3, pp. 123–134, 2020.

[42] P. Rollbusch and A. Magdeburg, “Gas holdup in two phase bubble columns at industrial processing conditions : effect of operating parameters, liquid properties and column scale,” 2016.

[43] A. Agarwal, W. J. Ng, and Y. Liu, “Principle and applications of microbubble and nanobubble technology for water treatment,” *Chemosphere*, vol. 84, no. 9, pp. 1175–1180, 2011, doi: 10.1016/j.chemosphere.2011.05.054.

[44] Y. Zhu, J. Wu, and R. Manasseh, “Rapid Measurement of Bubble Size in Gas-Liquid Flows Using a Bubble Detection Technique,” no. December, pp. 541–544, 2001.

[45] L. Cheng, T. Li, T. C. Keener, and J. Y. Lee, “A mass transfer model of absorption of carbon dioxide in a bubble column reactor by using magnesium hydroxide slurry,” *Int. J. Greenh. Gas Control*, vol. 17, pp. 240–249, 2013, doi: 10.1016/j.ijggc.2013.05.018.

[46] X. Jia, W. Hu, X. Yuan, and K. Yu, “Effect of surfactant type on interfacial area and liquid mass transfer for CO2 absorption in a bubble column,” *Chinese J. Chem. Eng.*, vol. 23, no. 3, pp. 476–481, 2015, doi: 10.1016/j.cjche.2014.11.027.

[47] H. Pashaei, A. Ghaemi, and M. Nasiri, “Modeling and experimental study on the solubility and mass transfer of CO_2 into aqueous DEA solution using a stirrer bubble column,” *RSC Adv.*, vol. 6, no. 109, pp. 108075–108092, 2016, doi: 10.1039/c6ra22589f.

[48] R. E. W. Jansson, *Electrochemical reaction engineering*, vol. 35, no. 9. 1980.

[49] Y. E. Kim, J. A. Lim, S. K. Jeong, Y. Il Yoon, S. T. Bae, and S. C. Nam, “Comparison of Carbon Dioxide Absorption in Aqueous MEA , DEA , TEA , and AMP Solutions,” vol. 34, no. 3, pp. 783–787, 2013.

[50] D. Gonzalez-Garza, R. Rivera-Tinoco, and C. Bouallou, “Comparison of ammonia, monoethanolamine, diethanolamine and methyldiethanolamine solvents to reduce CO_2 greenhouse gas emissions,” *Chem. Eng. Trans.*, vol. 18, pp. 279–284, 2009, doi:

10.3303/CET0918044.

[51] G. Yincheng, N. Zhenqi, and L. Wenyi, “Energy Procedia Comparison of removal efficiencies of carbon dioxide between aqueous ammonia and NaOH solution in a fine spray column,” *Energy Procedia*, vol. 4, pp. 512–518, 2011, doi: 10.1016/j.egypro.2011.01.082.

APPENDIXES

Appendix A: Design of bubble column reactor CSTR equation used

The design equation for the bubble column reactor is based on the CSTR design equation which is given from the general mole/material balance.

$(Rate\ of flow\ of\ j\ into\ the\ system) +$
$(rate\ of\ generation\ of\ j\ by\ chemical\ reaction\ within\ system) -$
$-(Rate\ of flow\ of\ j\ out\ the\ system) = (rate\ of\ accumulation\ of\ j\ within\ system)$

$$F_{jo} - F_j + \int_0^v r_j dV = \frac{dN_j}{dt} \tag{A.1}$$

When the general mole balance equation is applied to CSTR operated at a steady-state (i.e. condition do not change with time).

$$\frac{dN_j}{dt} = 0 \tag{A.2}$$

In which there are no spatial variations in the rate of reaction

$$\int_0^v r_j dV = V r_j \tag{A.3}$$

Then the above equation becomes

$$F_{jo} - F_j + V r_j = 0 \tag{A.4}$$

After rearranging it takes the familiar form known as the Design equation for a CSTR.

$$V = \frac{F_{jo} - F_j}{r_j} \tag{A.5}$$

This reactor volume equation is expressed in terms of the cross-sectional area and height of the reactor. So to arrange for the reactor height we consider the reactor is designed as a rectangular pipe whose volume is given as $V = LWH$.

$$LWH = \frac{F_{jo} - F_j}{r_j} \tag{A.6}$$

Then the arrangement for the height of the reactor is given as

$$H = \frac{1}{LW}\frac{F_{jo} - F_j}{r_j} \tag{A.7}$$

Appendix B: Calculation of dispersion number, $\frac{D}{UL}$

Then the Bubble column reactor designed will be assumed closed system, the mean and variance are evaluated numerically as was first done by van der Laan (1958) in the equation.

The meantime, for discrete data, is defined as

$$\dot{t} = \frac{\int_0^\infty tCdt}{\int_0^\infty Cdt} = \frac{\sum tiCi\Delta ti}{\sum Ci\Delta ti} \tag{B.1}$$

The variance is defined as

$$\sigma^2 = \frac{\sum(ti - \dot{t})^2 Ci\Delta ti}{\sum Ci\Delta ti} = \frac{\sum ti^2 Ci\Delta ti}{\sum Ci\Delta ti} - \dot{t}^2 \tag{B.2}$$

This equation is directly linked to the $\frac{D}{UL}$ as the following equation

$$\sigma_\theta^2 = \frac{\sigma_t^2}{\dot{t}^2} = 2\left(\frac{D}{UL}\right) - 2\left(\frac{D}{UL}\right)^2 (1 - e^{-uL/D}) \tag{B.3}$$

Appendix C: Drawing of Bubble Column Reactor

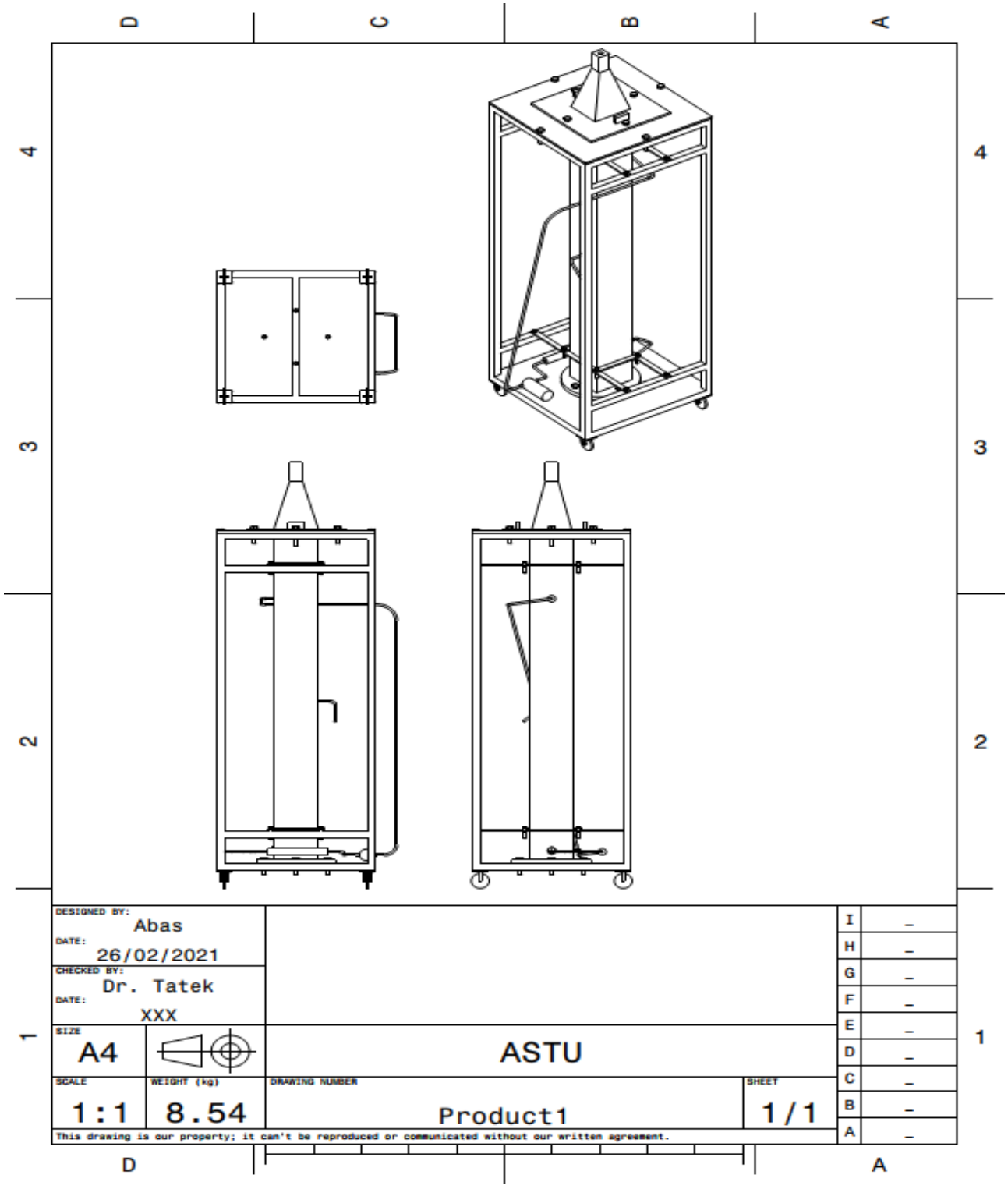

Appendix D: Assumptions for design of venture bubble generator

To estimate the geometrical parameters, the following assumptions were made

- ✓ Inlet flow rate = flow rate of feed pump, 1.5 L/min ($2.5*10^{-5}$ m^3/s)
- ✓ No height difference between the water inlet and throat ($Z_1 = Z_2$)
- ✓ The pressure at the inlet (P1) $= P_{atm} + \rho gH$ where H is the head of the pump
- ✓ Internal diameter = 6 mm for inlet and 3 mm for throat section of the venture
- ✓ Density of water ($\boldsymbol{\rho}_w$) = 1000kg/m^3

By taking the recycle pump flow rate, assumed above the velocity in the converging region (V_1) and throat tube (V_2) is calculated from the equation of continuity (3.3):

$$V1 = \frac{\mathrm{Q1}}{A_1} \tag{D.1}$$

Where

$$A_1 = \pi r_1^2 = 3.14 * (0.003)^2 = 2.83 * 10^{-5}\, m^2$$

$$A_2 = \pi r_2^2 = 3.14 * (0.0015)^2 = 0.7065 * 10^{-5}\, m^2$$

Then

$$V1 = \frac{\mathrm{Q1}}{A_1} = \frac{(2.5 * 10 - 5\ \mathrm{m3/s})}{2.83 * 10^{-5}\, m^2} = 0.8834 m/s$$

$$V2 = \frac{A_1 V_1}{A_2} = \frac{2.83 * 10^{-5}\, m^2 * 0.8834 m/s}{0.7065 * 10^{-5}\, m^2} = 3.5336 m/s$$

Then to calculate the value of Pressure at the inlet (P1) take the density of water 1000 kg/m^3

$$P1\ = P_{atm} + \rho gH = 101325pa + 1000\,\frac{\mathrm{kg}}{\mathrm{m3}} * \frac{9.81m}{s^2} * 3m = 130755pa = 1.29atm$$

The pressure at the throat (P_2) is calculated from equation (3.4).

$$P_2 = P_1 + \frac{1}{2} V_1^2 \rho (1 - (\frac{A_1}{A_2})^2)$$

$$P_2 = 130755pa\ + \frac{1}{2} * (\frac{0.8834m}{s})^2 * 1000\mathrm{kg/m3}(1 - (\frac{2.83 * 10^{-5}\, m^2}{0.7065 * 10^{-5}\, m^2})^2)$$

$$P_2 = 130755pa - 5870.92pa$$

$$P_2 = 124884.08pa = 1.23atm$$

Appendix E: Detail drawing of the venture bubble generator

Part 1

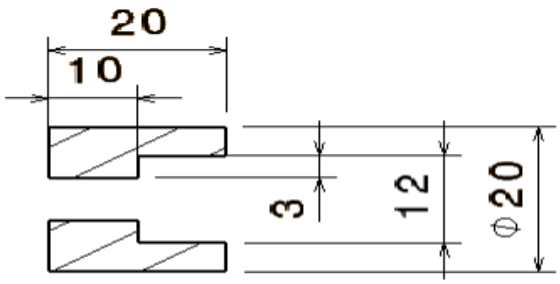

Part 2

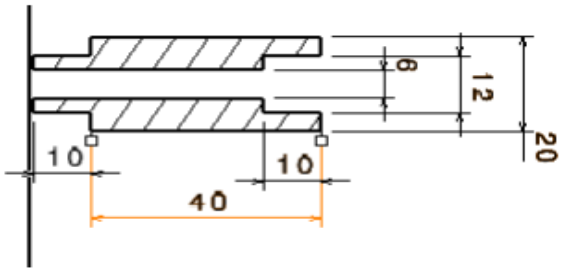

Part 3

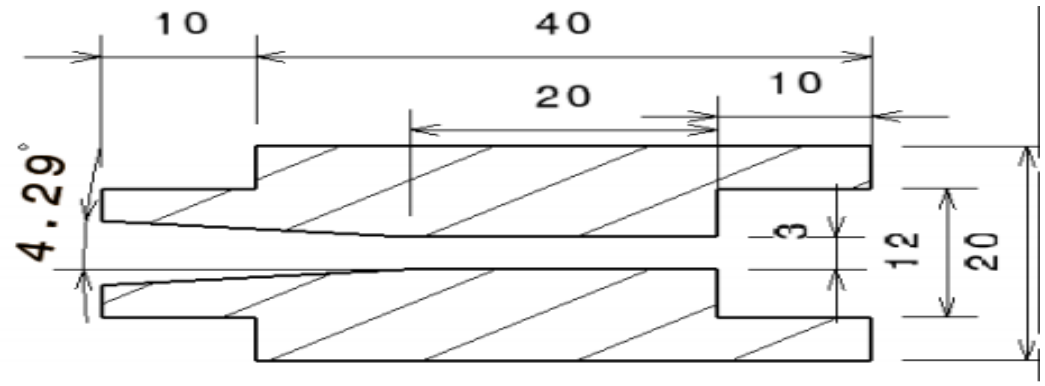

Part 4

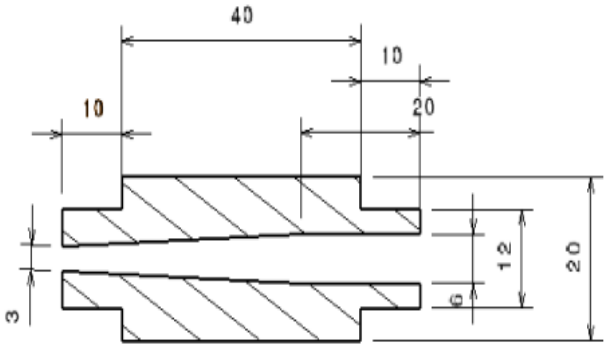

Part 5

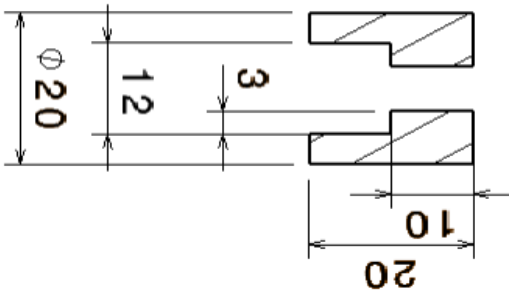

Appendix F: The Data of Area and diameters of individual bubbles from ImageJ Software.

	Area (mm^2)	D^2	Diameters in (mm)	Diameters in (μm)
1	3.53E-04	4.49E-04	0.021197	21.20
2	5.29E-04	6.74E-04	0.025962	25.96
3	5.46E-04	6.95E-04	0.026371	26.37
4	4.91E-04	6.26E-04	0.025017	25.02
5	4.58E-04	5.83E-04	0.024147	24.15
6	7.10E-04	9.04E-04	0.030068	30.07
7	4.41E-04	5.62E-04	0.023699	23.70
8	2.23E-04	2.84E-04	0.016839	16.84
9	3.86E-04	4.92E-04	0.022183	22.18
10	4.66E-04	5.94E-04	0.024367	24.37
11	0.002	2.55E-03	0.050475	50.48
12	4.07E-04	5.19E-04	0.022778	22.78
13	6.05E-04	7.70E-04	0.027755	27.75
14	5.42E-04	6.90E-04	0.026269	26.27
15	5.38E-04	6.85E-04	0.026167	26.17
16	0.001	1.27E-03	0.035692	35.69
17	5.21E-04	6.63E-04	0.025755	25.75
18	6.05E-04	7.70E-04	0.027755	27.75
19	4.24E-04	5.40E-04	0.023243	23.24
20	2.69E-04	3.42E-04	0.018501	18.50
21	7.31E-04	9.31E-04	0.030509	30.51
22	5.17E-04	6.58E-04	0.025651	25.65
23	4.54E-04	5.78E-04	0.024036	24.04
24	3.82E-04	4.87E-04	0.022062	22.06